

MASTER'S THESIS

Infall Velocity in Galaxy Clusters

Christoffer Bruun-Schmidt

Supervisor: Steen Harle Hansen
Dark Cosmology Centre, Niels Bohr Institute, University of Copenhagen
Juliane Maries Vej 30, 2100 Copenhagen O, Denmark

Date of submission: October 15, 2015

Abstract

This thesis consists of two separate parts. In the first part, I investigate the so called tethered galaxy problem, which concerns the motion of free particles in an eternally expanding universe. In particular, I try to analytically determine what happens to a particle removed from the Hubble flow according to currently favored theories. Will it for example rejoin the Hubble flow, or will it forever maintain its peculiar velocity through the expanding universe? So far, there have been different opinions about the correct answer, which is important for our understanding of the expansion of the universe. I find that the answer depends partly on how one mathematically defines what it means to rejoin the Hubble flow and partly on the dominant equation of state.

In the second part, I estimate the influence that the infall velocity in galaxy clusters has on the cluster dynamics and on the total mass profile of clusters in particular. When dealing with the dynamics of galaxy clusters, hydrostatic equilibrium is usually assumed, i.e. it is assumed that there is no infall velocity. However, most galaxy clusters are not yet fully equilibrated, and therefore this assumption is unjustifiable. I find that the influence of the infall velocity is non-negligible outside approximately one virial radius, and that the error associated with omitting it is as large as $\sim 15\%$ according to simulation data. Furthermore, I present a method for measuring the anisotropy parameter, β , the value of which can be used to put constraints on the collisionality of dark matter.

Contents

1	Introductory comments	3
2	Part 1: The tethered galaxy problem	3
2.1	The Robertson-Walker metric	4
2.2	Definitions	4
2.3	Examination of definitions	5
2.4	Discussion	9
2.5	Equation (2.3)	10
2.6	Remarks	11
2.7	Summary and conclusion	12
3	Part 2: Infall velocity in galaxy clusters	13
3.1	The standard equations of cluster dynamics	13
3.2	The generalized equations of cluster dynamics	15
3.3	Numerical simulations	16
3.3.1	The RAMSES simulation	17
3.3.2	The GADGET-3 simulation	17
3.4	Parameterizing the radial velocity	18
3.5	Influence of the infall velocity: The mass excess	22
3.6	Measuring β	25
3.6.1	Estimating the κ profile	27
3.6.2	Incomplete modelling of the gas physics?	28
3.7	Extracting the gas density and temperature from observations . .	31
3.7.1	X-ray observations	31
3.7.2	Deprojection ("onion peeling")	32
3.8	Discussion	34
3.8.1	The numerical simulations	34
3.8.2	The mass excess	34
3.8.3	The dark matter temperature	34
3.9	Summary and conclusion	37
4	References	38
	Appendix	40
A		40
B		41

C	42
D	43
E	47
F	50
G	56

1 Introductory comments

My thesis is divided into two separate parts. The first part concerns the tethered galaxy problem, while the second part concerns the infall velocity in galaxy clusters. Originally, I started working on the first project (part 1), but after a few months I ran into a dead end and therefore started working on the second project (part 2), which can be regarded as the "main project".

2 Part 1: The tethered galaxy problem

The conventional interpretation of the observed redshifts of galaxies is that space itself expands and that cosmological structures (although essentially static) are "carried" away from each other by this expansion.¹

In a popular analogy, space is represented by a rubber sheet being stretched. If one was to take this analogy literally it would imply that free particles in an expanding universe would always join the Hubble flow. However, in reality there is no rubber sheet - this is just an analogy that seems to fit well with reality due to observations. Barnes et al. 2006 set up the following thought experiment. A person is at rest on a large invisible rubber sheet (at rest in space) and observes an object moving away from him/her. The person can interpret this phenomenon in two equally correct ways: 1) The invisible rubber sheet is being stretched. 2) The sheet is at rest, and the object is moving across the sheet. Whether option 1 or option 2 is correct can be tested by dropping an object onto the sheet a certain distance away from the observer. If the sheet is being stretched, the dropped object would be carried away, but if the sheet is at rest, the dropped object would remain at rest as well, and thus one could conclude that the receding object must be moving across the sheet.

This thought experiment is similar to the tethered galaxy problem. Imagine two galaxies tethered together and thereby prevented from receding from each other. If the tether between the galaxies is cut, will the galaxies remain at rest, or will they move away from one another as a result of the Hubble flow? Intuitively, one would expect that only one of the two possibilities can be correct, but this is of course difficult to test experimentally. Attempts have been made to obtain an

¹In an alternative interpretation of the observed redshifts of galaxies, structures homogeneously and isotropically move away from each other through a static space. Although the expanding space interpretation is widely favored while the static space interpretation is generally regarded as being wrong, there are in fact no arguments justifying this conviction, which I explained in my Bachelor's thesis (The Expansion of the Universe).

answer analytically, and the generally most favored conclusion seems to be that the galaxies will join the Hubble flow. There are no clear arguments justifying this conclusion though, which will be explained below. One particular attempt to obtain the answer to the question analytically can be found in Barnes et al. 2006. In this paper, the authors set up seven mathematically different (but equally correct) definitions of what it means to "asymptotically join the Hubble flow", and for each of them, they determine whether a free particle will join the Hubble flow or not in an eternally expanding universe.

Below, I present four of their seven definitions², but firstly, for convenience, the Robertson-Walker metric is introduced.

2.1 The Robertson-Walker metric

The Robertson-Walker (RW) metric describes a spatially homogeneous and isotropic universe and relates the spacetime interval, ds , to the cosmic time, t , and the spherical comoving spatial coordinates; χ , θ and ϕ (χ being the radial coordinate while θ and ϕ are the tangential ones). The RW metric is given by

$$ds^2 = dt^2 - a^2(t) [d\chi^2 + S_k^2 (d\theta^2 + \sin^2 \theta d\phi^2)] . \quad (2.1)$$

Here, $a(t)$ is the scale factor determining whether the universe is expanding, contracting or static, and $S_k = \sin \chi, \chi, \sinh \chi$, for $k = +1, 0, -1$, where k is the spatial geometry parameter determining whether space is closed, flat or open, respectively. The speed of light, c , which usually appears squared in front of dt^2 , has been set to unity for convenience.

2.2 Definitions

Definition 1 ($\dot{\chi} \rightarrow 0$ as $t \rightarrow \infty$):

If a particle's velocity through coordinate space, $\dot{\chi} = \frac{d\chi}{dt}$, approaches zero as t approaches ∞ , the coordinate trajectory, $\chi(t)$, of the particle approaches a constant as $t \rightarrow \infty$. This means that the particle gradually slows down its motion through coordinate space and thus asymptotically joins the Hubble flow.

Definition 2 ($\chi \rightarrow \chi_\infty$ as $t \rightarrow \infty$):

If the coordinate trajectory, $\chi(t)$, of a particle approaches a constant, χ_∞ , as t

²This is sufficient for my purpose, since an examination including the remaining three definitions yields the same result and therefore only enhances the conclusion that will be drawn from the examination of the four selected definitions.

approaches ∞ , the particle gradually slows down and thus asymptotically joins the Hubble flow.

Definition 3 ($v_{\text{pec}} \rightarrow 0$ as $t \rightarrow \infty$):

The peculiar velocity of a particle is defined as $v_{\text{pec}} \equiv a(t)\dot{\chi}(t)$ (the scale factor at time t times the velocity relative to the Hubble flow). Meanwhile, proper distance is defined as the radial spacetime interval at constant time (i.e. $dt = d\theta = d\phi = 0$). With these conditions, the RW metric (equation (2.1)) yields the proper distance $r_p(t) = a(t)\chi(t)$. Taking the time derivative of the proper distance and using the product rule gives the proper velocity

$$\dot{r}_p = \dot{a}(t)\chi(t) + a(t)\dot{\chi}(t) = v_{\text{rec}} + v_{\text{pec}}, \quad (2.2)$$

where v_{rec} (the recession velocity) is the velocity of the Hubble flow. If I define the coordinate system so that $\chi(t) = 0$ at time t , then $v_{\text{rec}} = 0$, and thus the proper velocity of the particle is solely its peculiar velocity. Therefore, the peculiar velocity of a particle is its proper velocity relative to the Hubble flow. So in the case that v_{pec} of a particle approaches zero as t approaches ∞ , the particle must asymptotically join the Hubble flow.

Definition 4 ($\dot{r}_p \rightarrow v_{\text{rec}}$ as $t \rightarrow \infty$):

In the case that the proper velocity of a particle approaches its recession velocity (which is by definition the velocity of the Hubble flow) as t approaches ∞ , the particle must asymptotically join the Hubble flow.

2.3 Examination of definitions

If true, each of the mathematical definitions presented above implies that a free particle asymptotically will join the Hubble flow. Therefore, I will now examine all of the definitions closer to see if they actually do hold true in any eternally expanding universe.

Definition 1 ($\dot{\chi} \rightarrow 0$ as $t \rightarrow \infty$):

For purely radial particle motion, the following equation applies (Grøn & Elgarøy 2006):

$$\chi(t) = \chi_0 \pm \int \frac{1}{a\sqrt{1 + Ca^2}} dt, \quad (2.3)$$

where C is a positive constant, and χ_0 is the value of χ at $t = 0$. The time derivative of this is

$$\dot{\chi}(t) = \pm \frac{1}{a\sqrt{1+Ca^2}}, \quad (2.4)$$

but as $t \rightarrow \infty$ in an eternally expanding universe, a becomes very large, and thus I can infer the approximation $\sqrt{1+Ca^2} \approx \sqrt{Ca^2} = \sqrt{C}a$, so I get

$$\dot{\chi}(t) \approx \pm \frac{1}{a\sqrt{C}a} = \pm \frac{1}{\sqrt{C}a^2}. \quad (2.5)$$

Equation (2.5) shows that as $t \rightarrow \infty$, $\dot{\chi} \propto a^{-2} \rightarrow 0$ in an eternally expanding universe, so according to definition 1, any free particle in space will indeed asymptotically join the Hubble flow.

Definition 2 ($\chi \rightarrow \chi_\infty$ as $t \rightarrow \infty$):

Although looking similar, this definition is different from definition 1 for the following reason: If the derivative of a function approaches zero, it is not always the case that the function itself approaches a constant. $f(x) = \log(x)$ is an example of such a function. By use of the cosmological GR equations of motion, Barnes et al. show that when considering purely radial geodesics, there is no dependence on the curvature parameter, k . Therefore, one can without loss of generality, set $k = 0$ in the Friedmann equation, which then yields (see e.g. Ryden 2003)

$$a(t) = a_0 \left(\frac{t}{t_0} \right)^{2/(3+3\omega_i)}, \quad (2.6)$$

where a_0 is the scale factor at the present epoch, t_0 is the age of the universe and, ω_i is the sum of the equation of states of the components present in the universe. In an eternally expanding universe, $a(t) \rightarrow \infty$ as $t \rightarrow \infty$ by definition, and from equation (2.6), it is apparent that $a \propto t^{-\frac{3}{2}(1+\omega_i)}$. Therefore, for large t , the component with the most negative equation of state dominates the dynamics of the universe, and thus I can write an approximation for large t as

$$a(t) \approx a_0 \left(\frac{t}{t_0} \right)^{2/(3+3\omega_d)}, \quad (2.7)$$

where ω_d is the most dominant (most negative) equation of state.

Now, again using the approximation $\sqrt{1 + Ca^2} \approx \sqrt{C}a$ and substituting equation (2.7) into equation (2.3) while integrating from $t_0 = 1$ to t , I get

$$\begin{aligned}
\chi(t) &\approx \chi_0 \pm \int_{t_0}^t \frac{1}{\sqrt{C}a^2} dt' = \chi_0 \pm \frac{1}{\sqrt{C}} \int_1^t a^{-2} dt' \\
&= \chi_0 \pm \frac{1}{\sqrt{C}a_0} \int_1^t t'^{-4/(3+3\omega_d)} dt' = \chi_0 \pm \frac{1}{\sqrt{C}a_0} \int_1^t t'^{-2n} dt' \\
&= \chi_0 \pm \frac{1}{\sqrt{C}a_0} \left(\int_1^t t'^{-2n} dt' + \frac{1}{2n-1} \right) \\
&= \chi_0 \pm \frac{1}{\sqrt{C}a_0} \frac{1}{2n-1} \pm \frac{1}{\sqrt{C}a_0} \int_1^t t'^{-2n} dt' \\
&= \chi_f \pm \frac{1}{\sqrt{C}a_0} \int_1^t t'^{-2n} dt', \tag{2.8}
\end{aligned}$$

where $n = 2/(3 + 3\omega_d)$ and $\chi_f = \chi_0 \pm \frac{1}{\sqrt{C}a_0} \frac{1}{2n-1}$. So for χ to approach $\chi_f = \chi_\infty$ as t approaches ∞ , it is required that

$$2n > 1 \quad \Rightarrow \quad \omega_d < 1/3. \tag{2.9}$$

Otherwise the integral in equation (2.8) will diverge, and thus χ will diverge from χ_∞ when increasing t . Therefore, according to definition 2, a free particle in a universe dominated by an energy component with equation of state $\omega \geq 1/3$ will not join the Hubble flow.³

Definition 3 ($v_{\text{pec}} \rightarrow 0$ as $t \rightarrow \infty$):

Equation (2.5) shows that $\dot{\chi} \propto a^{-2}$, so I have that

$$v_{\text{pec}} \equiv a(t)\dot{\chi}(t) \propto a^{-1}, \tag{2.10}$$

and since a becomes large at large t , this means that $v_{\text{pec}} \rightarrow 0$ as $t \rightarrow \infty$. Therefore, according to definition 3, any free particle in space will asymptotically join the Hubble flow.

Definition 4 ($\dot{r}_p \rightarrow v_{\text{rec}}$ as $t \rightarrow \infty$):

Although looking similar, this definition is different from definition 3 for the following reason: If $\dot{r}_p = \dot{a}(t)\chi(t) + a(t)\dot{\chi}(t) = v_{\text{rec}} + v_{\text{pec}}$, and $v_{\text{pec}} \rightarrow 0$, it must be the case that $\dot{r}_p \rightarrow v_{\text{rec}}$, but if v_{rec} too approaches zero and does so as fast or

³Note that no substance with $\omega > 1/3$ is currently known.

faster than v_{pec} , this no longer applies. The condition for definition 4 to apply can be restated in the following way:

$$\begin{aligned} \dot{r}_{\text{p}} \rightarrow v_{\text{rec}} & \Rightarrow \frac{\dot{r}_{\text{p}}}{v_{\text{rec}}} \rightarrow 1 \Rightarrow \frac{v_{\text{rec}} + v_{\text{pec}}}{v_{\text{rec}}} \rightarrow 1 \\ & \Rightarrow \frac{v_{\text{pec}}}{v_{\text{rec}}} \rightarrow 0. \end{aligned} \quad (2.11)$$

This condition will be used in a moment. Meanwhile, using equation (2.8), I can write

$$\chi(t) \approx \chi_f \pm \frac{1}{\sqrt{C}a_0} \int^t t'^{-2n} dt = \chi_f \pm \frac{1}{\sqrt{C}a_0} \begin{cases} \frac{t^{1-2n}}{1-2n}, & \text{if } n \neq 1/2 \\ \ln(t), & \text{if } n = 1/2 \end{cases}. \quad (2.12)$$

Furthermore, I have that $v_{\text{rec}} = \dot{a}\chi$, where $\dot{a} \propto t^{n-1}$, since $a \propto t^{2/(3+3\omega_d)} = t^n$. Therefore, I can now write

$$v_{\text{rec}} \propto t^{n-1} \chi \propto t^{n-1} + \begin{cases} t^{-n}, & \text{if } n \neq 1/2 \\ t^{-1/2} \ln(t), & \text{if } n = 1/2 \end{cases}. \quad (2.13)$$

Now I examine what happens to $\frac{v_{\text{pec}}}{v_{\text{rec}}}$ as $t \rightarrow \infty$ for the three cases $n > 1/2$, $n = 1/2$ and $n < 1/2$. For the definition to hold, $\frac{v_{\text{pec}}}{v_{\text{rec}}}$ has to approach zero according to equation (2.11).

$n > 1/2$:

$$n > 1/2 \Rightarrow 2n - 1 > 0 \Rightarrow n - 1 > -n. \quad (2.14)$$

Therefore, the first term in equation (2.13) is the dominant one, so I have that $v_{\text{rec}} \propto t^{n-1}$. Equation (2.10) states that $v_{\text{pec}} \propto a^{-1} \propto t^{-n}$, so

$$\frac{v_{\text{pec}}}{v_{\text{rec}}} \propto \frac{t^{-n}}{t^{n-1}} \rightarrow 0 \quad \text{as } t \rightarrow \infty \quad (2.15)$$

in accordance with equation (2.11).

$n = 1/2$:

If $n = 1/2$, then $v_{\text{rec}} \propto t^{-1/2} + t^{-1/2} \ln(t)$, where $t^{-1/2} < t^{-1/2} \ln(t)$, so the second term is the dominant one, and thus I have that $v_{\text{rec}} \propto t^{-1/2} \ln(t)$. Furthermore, $v_{\text{pec}} \propto t^{-n} = t^{-1/2}$, so

$$\frac{v_{\text{pec}}}{v_{\text{rec}}} \propto \frac{t^{-1/2}}{t^{-1/2} \ln(t)} \rightarrow 0 \quad \text{as } t \rightarrow \infty \quad (2.16)$$

again in accordance with equation (2.11).

$n < 1/2$:

If $n < 1/2$, then $n - 1 < -n$, simply by reversing the sign in equation (2.14), and thus the first term in equation (2.13) is now the dominant one, which implies that $v_{\text{rec}} \propto t^{-n}$. Meanwhile, $v_{\text{pec}} \propto t^{-n}$, so

$$\frac{v_{\text{pec}}}{v_{\text{rec}}} \propto \frac{t^{-n}}{t^{-n}} \rightarrow 1 \quad \text{as } t \rightarrow \infty. \quad (2.17)$$

So when $n < 1/2$, or equally, when $\omega_d > 1/3$, definition 4 fails. Therefore, according to definition 4, a free particle in a universe dominated by an energy component with equation of state $\omega > 1/3$ will not join the Hubble flow.

2.4 Discussion

Do free particles in space asymptotically join the Hubble flow? Due to the rubber sheet analogy of space, one would intuitively expect the answer to be yes, but in this project, I have (on the basis of Barnes et al. 2006) investigated the question analytically by considering four mathematical definitions of what it means to "asymptotically join the Hubble flow".

According to definitions 1 and 3, free particles in any eternally expanding universe will asymptotically join the Hubble flow. However, according to definitions 2 and 4, particles will join the Hubble flow only in universes that comply with certain conditions depending on the equation of state of the dominant energy component. For example, according to definition 2, particles will join the Hubble flow in a matter dominated universe ($\omega = 0$), while they will fail to do this in a radiation dominated universe ($\omega = 1/3$).

In order to justify a conclusion that "free particles in an eternally expanding universe will join the Hubble flow" all mathematical definitions of the phrase (including those that are not mentioned in this document) would have to be met, and since this is not the case, one cannot make this conclusion.

Our initial thought was that this ambiguity of the answer could be caused by a flaw in the mathematical analysis, since it intuitively makes little sense that, whether a free particle in an eternally expanding universe joins the Hubble flow or not may depend on whether the universe is dominated by matter or radiation. Therefore, I decided to go backwards through the calculations to "search" for an error.

2.5 Equation (2.3)

In the mathematical definitions presented above, the equation describing radial particle motion (equation (2.3)) is the key equation, since it is part of each definition. Thus, I will now (on the basis of Grøn & Elgarøy 2006) derive this equation in order to determine if it is in fact correct. I start out with the general relativistic equation describing the motion of a free particle, namely the geodesic equation given by

$$\frac{d^2 x^\mu}{d\tau^2} + \Gamma_{\nu\sigma}^\mu \frac{dx^\nu}{d\tau} \frac{dx^\sigma}{d\tau} = 0. \quad (2.18)$$

Here, τ is the proper time, μ , ν and σ are spacetime indices, and $\Gamma_{\nu\sigma}^\mu$ is the Christoffel symbol given by

$$\Gamma_{\nu\sigma}^\mu = \frac{1}{2} g^{\mu\rho} \left[\frac{\partial g_{\sigma\rho}}{\partial x^\nu} + \frac{\partial g_{\rho\nu}}{\partial x^\sigma} - \frac{\partial g_{\nu\sigma}}{\partial x^\rho} \right], \quad (2.19)$$

where ρ too is a spacetime index, and $g_{\mu\nu}$ is the metric tensor:

$$g_{\mu\nu} = \begin{pmatrix} -c^2 & 0 & 0 & 0 \\ 0 & a^2 & 0 & 0 \\ 0 & 0 & 0 & 0 \\ 0 & 0 & 0 & 0 \end{pmatrix}, \quad (2.20)$$

$$g^{\mu\nu} = (g_{\mu\nu})^{-1} = \begin{pmatrix} -c^{-2} & 0 & 0 & 0 \\ 0 & a^{-2} & 0 & 0 \\ 0 & 0 & 0 & 0 \\ 0 & 0 & 0 & 0 \end{pmatrix}. \quad (2.21)$$

The only non-vanishing Christoffel symbols are $\Gamma_{\chi t}^\chi$, $\Gamma_{t\chi}^\chi$ and $\Gamma_{\chi\chi}^t$:

$$\Gamma_{\chi t}^\chi = \Gamma_{t\chi}^\chi = \frac{\dot{a}}{a}, \quad \Gamma_{\chi\chi}^t = \frac{a\dot{a}}{c^2}. \quad (2.22)$$

Using equation (2.22), the geodesic equation yields

$$\frac{d^2 \chi}{d\tau^2} = -2 \frac{\dot{a}}{a} \frac{\dot{\chi}}{\dot{\tau}^2}, \quad \frac{d^2 t}{d\tau^2} = -\frac{a\dot{a}}{c^2} \frac{\dot{\chi}^2}{\dot{\tau}^2}. \quad (2.23)$$

See appendix A for a derivation of equations (2.22) and (2.23).

Now I want to find an expression for $\ddot{\chi} = \frac{d\dot{\chi}}{dt}$, where $\dot{\chi} = \frac{d\chi/d\tau}{dt/d\tau}$, and the expression is (see appendix B for details)

$$\ddot{\chi} = \frac{d\dot{\chi}}{dt} = \frac{d}{dt} \left(\frac{d\chi/d\tau}{dt/d\tau} \right) = \dot{\tau}^2 \left(\frac{d^2 \chi}{d\tau^2} - \dot{\chi} \frac{d^2 t}{d\tau^2} \right). \quad (2.24)$$

Substituting equation (2.23) into equation (2.24) yields

$$\ddot{\chi} = \dot{\tau}^2 \left(-2 \frac{\dot{a}}{a} \frac{\dot{\chi}}{\dot{\tau}^2} + \dot{\chi} \frac{a\dot{a}}{c^2} \frac{\dot{\chi}^2}{\dot{\tau}^2} \right) = \frac{a\dot{a}}{c^2} \dot{\chi}^3 - 2 \frac{\dot{a}}{a} \dot{\chi}. \quad (2.25)$$

I now introduce the dimensionless variable $y = c^2/\dot{\chi}^2$. In terms of y , I get $\dot{\chi} = c/\sqrt{y}$ and $\ddot{\chi} = c \frac{d}{dt} \left(\frac{1}{\sqrt{y}} \right) = -\frac{c\dot{y}}{2y^{3/2}}$, so equation (2.25) becomes (see appendix C for details)

$$\dot{y} - y \frac{d}{dt} (\ln a^4) = -\frac{da^2}{dt}. \quad (2.26)$$

A solution to equation (2.26) is

$$y = a^2 + e^K a^4, \quad (2.27)$$

where K is a constant. That equation (2.27) is in fact a solution to equation (2.26) has been checked by substituting equation (2.27) into equation (2.26). Since K is a constant, $C \equiv e^K$ is a positive constant. If I substitute $y = c^2/\dot{\chi}^2$ into equation (2.27), I get

$$\begin{aligned} \frac{c^2}{\dot{\chi}^2} = a^2 + Ca^4 \quad \Rightarrow \quad \dot{\chi}^2 = c^2 (a^2 + Ca^4)^{-1} \quad \Rightarrow \\ \dot{\chi} = \pm c (a^2 + Ca^4)^{-1/2}. \end{aligned} \quad (2.28)$$

Integrating equation (2.28) and setting the speed of light, c , to unity, yields

$$\chi(t) = \chi_0 \pm \int \frac{1}{a\sqrt{1+Ca^2}} dt, \quad (2.29)$$

which is indeed identical to equation (2.3). That the equation is in fact correct, presupposes that the geodesic equation is correct, since this is the equation from which I started the derivation. Therefore, for the sake of completeness, a derivation of the geodesic equation can be found in appendix D.

2.6 Remarks

All the definitions given in section 2.2 are mathematical translations of what it means to asymptotically join the Hubble flow. Definition 1, for example, says that as time goes, the peculiar velocity of a free particle (or a previously tethered galaxy) should asymptotically approach zero, while definition 2 says that as time goes, the coordinate trajectory of a free particle should asymptotically approach

a constant. Both of these mathematical translations intuitively (in my opinion) make sense, since if a particle gradually slows down its motion through coordinate space, it gradually comes closer to purely follow the Hubble flow. However, I have a minor issue with the fact that Barnes et al., without further comments, base their definitions on the assumption that free particles in an eternally expanding universe will asymptotically join the Hubble flow. For instance, one could just as easily have assumed that the peculiar velocity of a free particle in such a universe would forever remain constant. According to this scenario, what happens when the tether between two galaxies is cut could depend on whether the expansion (or in theory the contraction) of the universe is constant or accelerating. Whether or not the correct scenario is assumed is not the most important aspect though, when one wants to explore what would happen in reality, since in this case, it is the mathematical analysis (which should yield the same result regardless of the presumptions) that is conclusive.

2.7 Summary and conclusion

Whether a free particle in an eternally expanding universe will asymptotically join the Hubble flow or not (or whether mutually tethered galaxies recede from each other when the tether is cut) is an open question to which it is apparently difficult to obtain a clear answer. According to section 2.3 above, the answer depends on how one mathematically defines what it means to asymptotically join the Hubble flow, and whether the particular universe is dominated by e.g. matter or radiation. In order to obtain a clear answer, each definition should yield the same result regardless of the dominant component of the universe, and since this is not the case, I investigated whether the derivation of the equation leading to the ambiguous answer (equation (2.3)) is in fact correct and found that it is (section 2.5). Therefore, I have to conclude that, according to my examination, the answer to the question of whether a free particle will asymptotically join the Hubble flow or not in an eternally expanding universe seems to be truly ambiguous, and that a clear answer apparently cannot be obtained from a purely mathematical analysis.

3 Part 2: Infall velocity in galaxy clusters

The main objective of this second part of the project is to estimate the influence that the infall velocity in galaxy clusters has on the cluster dynamics. Galaxy clusters are the largest gravitationally bound structures in the universe, and they consist of an extended dark matter (DM) halo, the X-ray emitting intracluster medium (ICM) and galaxies. When dealing with the dynamics of galaxy clusters, one generally uses the equation of hydrostatic equilibrium for the baryonic matter and the Jeans equation for the dark matter.

3.1 The standard equations of cluster dynamics

In this section, I introduce the standard equations describing the dynamics of galaxy clusters, i.e. the equation of hydrostatic equilibrium and the Jeans equation. The equation of hydrostatic equilibrium can be derived from the Euler equation describing adiabatic and inviscid flows given by (see e.g. Binney & Tremaine 2008)

$$\frac{\partial \mathbf{v}}{\partial t} + (\mathbf{v} \cdot \nabla) \mathbf{v} = -\frac{1}{\rho} \nabla P - \nabla \Phi, \quad (3.1)$$

where $\mathbf{v} = (\bar{v}_r, \bar{v}_\theta, \bar{v}_\phi)$ is the velocity vector, $\nabla = (\partial_r, \partial_\theta, \partial_\phi)$ is the spatial gradient, ρ is the density, P is the pressure, and Φ is the gravitational potential. The condition of hydrostatic equilibrium presupposes that the thermal pressure of the gas balances the clusters gravitational potential, which means that there is no net radial streaming motion, i.e. $\bar{v}_r = 0$. In addition, it will be assumed that there are no net rotational streaming motions, i.e. $\bar{v}_\theta = \bar{v}_\phi = 0$. This is a reasonable assumption as shown in Bullock et al. 2001. Hydrostatic equilibrium also means that the system is in a steady state, whereby all time gradients vanish. If in addition, the system is spherical, all angular gradients vanish, which means that $\nabla = \partial_r$. Furthermore, assuming that the gas in the system can be regarded as an ideal gas, equation (3.1) can be rewritten as (see appendix E for details)

$$\frac{\partial \Phi(r)}{\partial r} = \frac{GM(r)}{r^2} = -\frac{k_B T}{\mu m_H r} \left(\frac{\partial \ln \rho}{\partial \ln r} + \frac{\partial \ln T}{\partial \ln r} \right), \quad (3.2)$$

where M is the total mass of the galaxy cluster, T is the gas temperature, ρ is the gas density, G is the gravitational constant, k_B is the Boltzmann constant, μ is the mean molecular weight, and m_H is the mass of a hydrogen atom. Equation (3.2) is known as the equation of hydrostatic equilibrium.

The collisionless analog to the equation of hydrostatic equilibrium is called the Jeans equation, and it can be obtained from the collisionless Boltzmann equation describing the statistical behavior of collisionless systems, which in spherical coordinates reads (see e.g. Binney & Tremaine 2008)

$$\begin{aligned} \frac{\partial f}{\partial t} + p_r \frac{\partial f}{\partial r} + \frac{p_\theta}{r^2} \frac{\partial f}{\partial \theta} + \frac{p_\phi}{r^2 \sin^2 \theta} \frac{\partial f}{\partial \phi} - \left(\frac{\partial \Phi}{\partial r} - \frac{p_\theta^2}{r^3} - \frac{p_\phi^2}{r^3 \sin^2 \theta} \right) \frac{\partial f}{\partial p_r} \\ - \left(\frac{\partial \Phi}{\partial \theta} - \frac{p_\phi^2 \cos \theta}{r^2 \sin^3 \theta} \right) \frac{\partial f}{\partial p_\theta} - \frac{\partial \Phi}{\partial \phi} \frac{\partial f}{\partial p_\phi} = 0, \end{aligned} \quad (3.3)$$

where f is the distribution function, p_r , p_θ and p_ϕ are the canonical momenta, and Φ is again the gravitational potential. For a spherical system in a steady state, the terms involving ∂_t , ∂_θ and ∂_ϕ will vanish. The spherical velocity components feature in equation (3.3) via the relations $p_r = v_r$, $p_\theta = r v_\theta$ and $p_\phi = r \sin \theta v_\phi$, and if each mean velocity component is neglected (i.e. if $\bar{v}_r = \bar{v}_\theta = \bar{v}_\phi = 0$), equation (3.3) can be rewritten as (see appendix F for details)

$$-\nu \frac{\partial \Phi(r)}{\partial r} = \frac{\partial}{\partial r} (\nu \sigma_r^2) + 2 \frac{\beta}{r} \nu \sigma_r^2, \quad (3.4)$$

where ν is the DM number density, σ_r is the radial velocity dispersion, and

$$\beta \equiv 1 - \frac{\sigma_\theta^2 + \sigma_\phi^2}{2\sigma_r^2} \quad (3.5)$$

is the anisotropy parameter, where σ_θ and σ_ϕ are the tangential velocity dispersions. The anisotropy parameter expresses the degree of velocity anisotropy in clusters. The value of β can vary from $-\infty$, corresponding to perfectly circular orbits ($\sigma_r = 0$), to 1, corresponding to perfectly radial orbits ($\sigma_\theta = \sigma_\phi = 0$). When $\sigma_r = \sigma_\theta = \sigma_\phi$, the system is isotropic (i.e. $\beta = 0$). Equation (3.4) is known as the Jeans equation, which can be rewritten as

$$\frac{\partial \Phi(r)}{\partial r} = \frac{GM(r)}{r^2} = -\frac{\sigma_r^2}{r} \left(\frac{\partial \ln \nu}{\partial \ln r} + \frac{\partial \ln \sigma_r^2}{\partial \ln r} + 2\beta \right). \quad (3.6)$$

A derivation of equation (3.6) is given in appendix F.

Equation (3.2) and equation (3.6) both yield the total mass profile of a galaxy cluster given the assumptions of spherical symmetry, a steady state and hydrostatic equilibrium. These assumptions are reasonable within ~ 1 virial radius⁴

⁴The virial radius of a galaxy cluster is the radius within which the mean density of the cluster is 200 times the critical density of the universe.

(r_v) , which will be shown later. However, in the outer parts (for $r \gtrsim 1 r_v$), even clusters that appear relaxed can have a non-zero infall velocity, and thus, depending on the magnitude of this velocity, the assumption of hydrostatic equilibrium may not be valid, and it could lead to wrong estimates of cluster masses. Therefore, I will estimate the influence that the infall velocity has on the total cluster mass profile. This will be done using data from numerical simulations. First though, I introduce the generalized equations of the cluster dynamics, corresponding to equations (3.2) and (3.6), in which radial streaming motions are not neglected.

3.2 The generalized equations of cluster dynamics

If one retains the radial velocity component in the Euler equation given by equation (3.1) and terms involving the time derivative but still assumes spherical symmetry, equation (3.2) becomes (see appendix E for details)

$$\begin{aligned} \frac{\partial \Phi(r)}{\partial r} &= -\frac{k_B T}{\mu m_H r} \left(\frac{\partial \ln \rho}{\partial \ln r} + \frac{\partial \ln T}{\partial \ln r} \right) - \left(\bar{v}_r \frac{\partial \bar{v}_r}{\partial r} + \frac{\partial \bar{v}_r}{\partial t} \right) \\ &= -\frac{k_B T}{\mu m_H r} \left(\frac{\partial \ln \rho}{\partial \ln r} + \frac{\partial \ln T}{\partial \ln r} \right) \\ &\quad - \left(\bar{v}_p \frac{\partial \bar{v}_p}{\partial r} + H \left(\bar{v}_p + r \frac{\partial \bar{v}_p}{\partial r} \right) - q H^2 r + \frac{\partial \bar{v}_p}{\partial t} \right). \end{aligned} \quad (3.7)$$

Here, I have used that $\bar{v}_r = Hr + \bar{v}_p$, where $H(t)$ is the Hubble parameter, and $\bar{v}_p(r, t)$ is the mean radial peculiar velocity component. I have also used that $H = \frac{\partial H}{\partial t} = -(q+1)H^2$, where $q = -\frac{\ddot{a}a}{\dot{a}^2}$ is the so called deceleration parameter⁵ describing the acceleration of the expanding space, where $a(t)$ is the scale factor.

Furthermore, since I am now considering relatively large distances, the underlying cosmology should also be taken into account. In addition to being subject to its own gravitational potential, the outer parts of a galaxy cluster is also subject to an attractive potential resulting from the background density of the universe (ρ_b) and a repulsive potential resulting from the cosmological constant (Λ). Including these contributions, the total potential gradient becomes (see e.g. Peebles 1980)

$$\frac{\partial \Phi(r)}{\partial r} = \frac{GM(r)}{r^2} + \frac{4\pi}{3} G \rho_b r - \frac{1}{3} \Lambda r. \quad (3.8)$$

⁵The name is historical. It could more appropriately be named "the acceleration parameter".

Using equation (3.8), equation (3.7) can be rewritten as

$$\begin{aligned}
\frac{GM(r)}{r^2} &= -\frac{k_B T}{\mu m_H r} \left(\frac{\partial \ln \rho}{\partial \ln r} + \frac{\partial \ln T}{\partial \ln r} \right) - \left(\bar{v}_r \frac{\partial \bar{v}_r}{\partial r} + \frac{\partial \bar{v}_r}{\partial t} \right) - q H^2 r \\
&= -\frac{k_B T}{\mu m_H r} \left(\frac{\partial \ln \rho}{\partial \ln r} + \frac{\partial \ln T}{\partial \ln r} \right) \\
&\quad - \left(\bar{v}_p \frac{\partial \bar{v}_p}{\partial r} + H \left(\bar{v}_p + r \frac{\partial \bar{v}_p}{\partial r} \right) + \frac{\partial \bar{v}_p}{\partial t} \right). \tag{3.9}
\end{aligned}$$

Equation (3.9) is the new generalized equation replacing the equation of hydrostatic equilibrium. A derivation of this equation is given in appendix E.

Meanwhile, if one retains the radial velocity component in the collisionless Boltzmann equation given by equation (3.3) and terms involving the time derivative but still assumes spherical symmetry and in addition uses equation (3.8) for the gravitational potential, equation (3.6) becomes (see appendix F for details)

$$\begin{aligned}
\frac{GM(r)}{r^2} &= -\frac{\sigma_r^2}{r} \left(\frac{\partial \ln \nu}{\partial \ln r} + \frac{\partial \ln \sigma_r^2}{\partial \ln r} + 2\beta \right) - \left(\tilde{v}_r \frac{\partial \tilde{v}_r}{\partial r} + \frac{\partial \tilde{v}_r}{\partial t} \right) - q H^2 r \\
&= -\frac{\sigma_r^2}{r} \left(\frac{\partial \ln \nu}{\partial \ln r} + \frac{\partial \ln \sigma_r^2}{\partial \ln r} + 2\beta \right) \\
&\quad - \left(\tilde{v}_p \frac{\partial \tilde{v}_p}{\partial r} + H \left(\tilde{v}_p + r \frac{\partial \tilde{v}_p}{\partial r} \right) + \frac{\partial \tilde{v}_p}{\partial t} \right). \tag{3.10}
\end{aligned}$$

Note that I have used a tilde instead of a bar when writing the mean radial and peculiar velocity in order to clarify that the DM velocity is in general different from the gas velocity. Equation (3.10) is the new generalized equation replacing the standard Jeans equation.

In order to be able to estimate the influence that the infall velocity has on the total cluster mass, I need to know both of these parameters. Unfortunately, they cannot be obtained from direct observations, so instead I do the second best thing and use simulation data.

3.3 Numerical simulations

I use the data from two different numerical simulations of the formation of galaxy clusters in the standard Λ CDM cosmology to parameterize the infall velocity in galaxy clusters and assess its influence on the total cluster mass. In particular, one simulation was run with the adaptive mesh refinement (AMR) code RAMSES (Teyssier 2002), while the other simulation was run with the smoothed

particle hydrodynamics (SPH) code GADGET-3, which is an improved version of the GADGET-2 code (Springel 2005). These two simulation techniques are completely different from each other, and thus they should provide a good check for systematic effects. Throughout the thesis, I refer to the former as the RAMSES simulation and to the latter as the GADGET-3 simulation.

3.3.1 The RAMSES simulation

I first analyze a sample of 51 cluster sized halos (all with total mass larger than $10^{14}M_{\odot}$) extracted from a simulation performed by Martizzi, Mohammed, Teyssier and Moore. All details of the simulation can be found in Martizzi et al. 2014. The simulation was run with the AMR code RAMSES and follows the evolution of large-scale structure within a box of size $144h^{-1}$ Mpc. The cosmological parameters are $h = 0.704$, $\sigma_8 = 0.809$, $n_s = 0.963$, $\Omega_{\Lambda} = 0.728$, $\Omega_m = 0.272$ and $\Omega_b = 0.045$. Here, the Hubble constant is given by $H_0 = 100 h \text{ km s}^{-1} \text{ Mpc}^{-1}$, σ_8 is the rms mass fluctuation at the present epoch in a sphere of radius $8 h^{-1}$ Mpc, n_s is the spectral index of primordial density perturbations, and Ω_{Λ} , Ω_b and Ω_m are the density parameters of the cosmological constant, the baryonic matter and the baryonic matter plus the dark matter, respectively. The 51 halos were re-simulated three times; one time considering only dark matter and two times including baryons. Both runs including baryons include models for gas cooling, star formation, supernovae feedback and metal enrichment, while AGN feedback was only included in one of them.

3.3.2 The GADGET-3 simulation

The second sample consists of 29 cluster sized halos (most of which have a total mass larger than $10^{15}M_{\odot}$) extracted from re-simulations of a parent simulation presented in Bonafede et al. 2011. All details of the parent simulation can be found in Bonafede et al. 2011, while the details of the resimulations can be found in Planelles et al. 2013. The simulations were run with the TREEPM-SPH code GADGET-3, and the cosmological parameters are $h = 0.72$, $\sigma_8 = 0.8$, $n_s = 0.96$, $\Omega_{\Lambda} = 0.76$, $\Omega_m = 0.24$ and $\Omega_b = 0.04$. Three different sets of re-simulations were run: 1) A non-radiative hydrodynamical set. 2) A hydrodynamical set including effects of cooling, star formation and supernovae feedback. 3) A set including AGN feedback but otherwise similar to set 2.

3.4 Parameterizing the radial velocity

Now I want to estimate the influence that the mean radial velocity has on the total cluster mass, but as mentioned, to do this, the radial velocity first needs to be parameterized, so it can be handled as an analytic function in equations (3.9) and (3.10).

Figure 1 displays the mean radial peculiar velocity component relative to the circular velocity at the virial radius given by $v_v = \sqrt{GM_v/r_v}$, where M_v is the mass within the virial radius, r_v . The upper plot represents the RAMSES simulation which extends to $2r_v$, while the lower one represents the GADGET-3 simulation which (unfortunately) only extends to $\sim 1.3r_v$. In the RAMSES plot, the radial peculiar velocity of the dark matter and that of the gas seem to be almost identical, while the gas component is generally slightly less negative than the DM component in the GADGET-3 plot. It is not quite obvious why the magnitude of the radial velocity of the dark matter is almost equal to the magnitude of the radial velocity of the gas, since there is great difference between the ways that DM particles and baryonic particles give off energy. For instance, infalling baryonic particles primarily lose their energy in the form of radiation due to internal collisions, while DM particles lose their energy non-radiatively primarily due to dynamical friction and violent relaxation.

Figure 2 illustrates the difference between the peculiar velocity of the dark matter and that of the gas for both the RAMSES simulation (red) and the GADGET-3 simulation (blue). In particular, the quantities plotted are $(\tilde{v}_p - \bar{v}_p)/v_v$ (upper plot) and $(\tilde{v}_p - \bar{v}_p)/(\tilde{v}_p + \bar{v}_p)$ (lower plot). The values of these two quantities are not exactly zero (which would ideally be the case if the two velocity components were identical), but the deviation from zero is so small that it is difficult to account for in practice. Thus, I will throughout the thesis assume that $\tilde{v}_p = \bar{v}_p$, i.e. that the radial velocity profile of the dark matter and that of the gas are identical. In particular, I treat the peculiar velocity as an analytic function of radius given by

$$f\left(\frac{r}{r_v}\right) = -\alpha \left[\left(\left(\frac{r}{r_v}\right)^{-a} + C \left(\frac{r}{r_v}\right)^b \right)^{1/a} - D \right]^{-1}, \quad (3.11)$$

where α , a , b , C and D are the free parameters. For both the RAMSES plot and the GADGET-3 plot, I have given the parameters the following values: $\alpha = 0.12655906$, $a = 12.8245615$, $b = 0.5a$, $C = 2.2179 \cdot 10^{-6}$ and $D = 0.31763796$. These values are close to the ones presented in Falco et al. 2013, and they best match the RAMSES plot, but they also provide a decent fit to the GADGET-3

plot as seen in Figure 1.

In its innermost region, a galaxy cluster is fully equilibrated, i.e. $\bar{v}_r = 0$. This implies that $\bar{v}_p(r, t) \approx -Hr$ for $r \ll r_v$. In equation (3.11), this is accounted for by the term proportional to r (the leftmost term). In Figure 1, it is also apparent that in the innermost region, \bar{v}_p is approximately linear as it should be.

Far from the center (although close enough for gravity to dominate the Hubble expansion), where clusters are non-equilibrated, matter is falling towards the center almost freely, since in this region there are virtually no collisions, dynamical friction or any other slowing effects. Therefore, in this entire region, due to conservation of energy, the sum of the kinetic energy and the potential energy should equal a constant as the matter is falling in. In general, the potential of a particle of mass m , located at a radius r , from a point mass⁶ M , is defined as the work done by the gravitational field bringing the unit mass in from infinity⁷, and it is given by

$$\Phi = -\frac{GM}{r}. \quad (3.12)$$

At infinite radius, $\Phi = 0$, and Φ becomes more and more negative as r is decreased. Meanwhile, the kinetic energy of the particle of mass m is given by

$$K = \frac{1}{2}mv^2, \quad (3.13)$$

where v is the velocity of the particle. At infinite radius, $v = 0$, which implies that $K = 0$ at infinity. This implies that at all radii, $K + \Phi = 0$, and thus that $K = -\Phi$. This, combined with equation (3.12) and equation (3.13), allows me to write

$$\frac{1}{2}mv^2 = \frac{GM}{r} \quad \Rightarrow \quad v = \sqrt{\frac{2GM}{rm}} \propto r^{-1/2}. \quad (3.14)$$

In equation (3.11), this "conservation of energy" or "free fall" term is accounted for by the term proportional to $r^{-1/2}$ (the term that is multiplied by C).

The constants C and D feature in equation (3.11) to make sure that the fitted curve in Figure 1 decreases by the "right" amount when approaching $2r_v$.

⁶The galaxy cluster can be regarded as a point mass in the described region, since essentially all of its mass lies within the radius at which the particle is located.

⁷In this case infinity is a bad term, since particles at sufficiently large radii would be carried away by the Hubble flow. Therefore, in this scenario, infinity is somewhere far away from the cluster center, but where the gravitational potential of the cluster still overcomes the Hubble expansion. Today, this is at $\sim 3.5r_v$ for a cluster of mass $M \approx 10^{14}M_\odot$ (Cuesta et al. 2008).

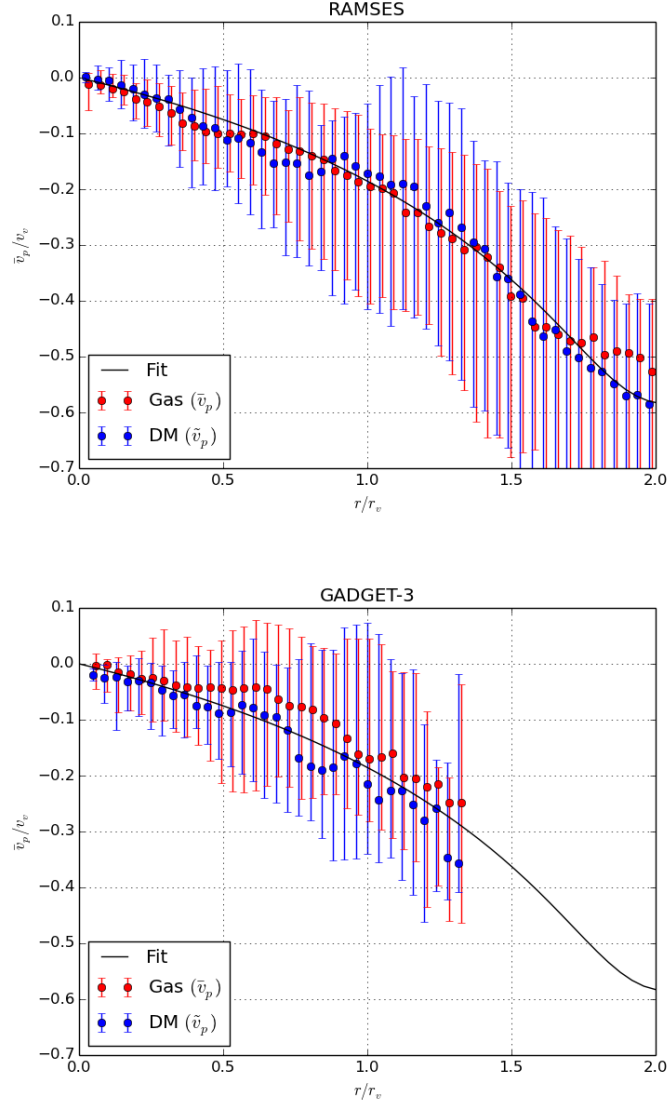


Figure 1: The mean radial peculiar velocity relative to v_v (the circular velocity at the virial radius) as a function of radius. The upper plot represents the RAMSES simulation, while the lower one represents the GADGET-3 simulation. In both cases, the red and blue filled circles represent the median value (of all the clusters) of the mean peculiar velocity of the gas (\bar{v}_p) and the dark matter (\tilde{v}_p) respectively, and the vertical lines are 1σ error bars. The black solid lines represent the fit given by equation (3.11). Note that the gas part has been displaced slightly to the right in both plots for visual purposes.

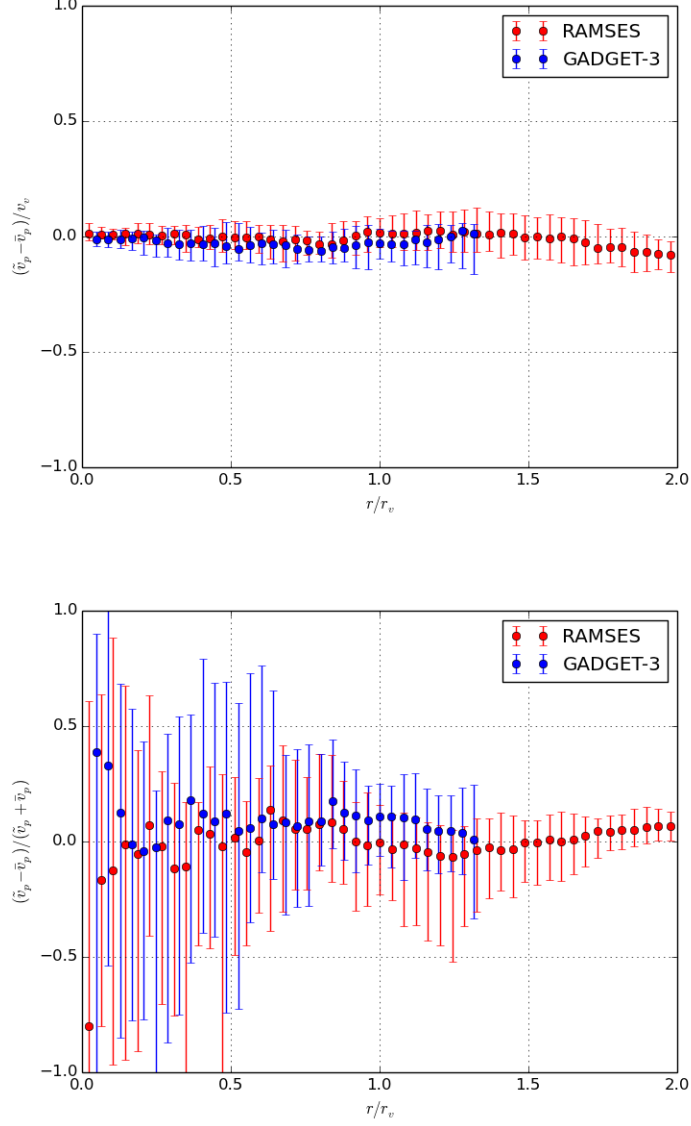


Figure 2: Illustration of the difference between the mean peculiar velocity of the dark matter and that of the gas given by \tilde{v}_p and \bar{v}_p respectively. The upper plot shows the quantity $(\tilde{v}_p - \bar{v}_p)/v_v$ plotted as a function of radius, while the lower plot shows the quantity $(\tilde{v}_p - \bar{v}_p)/(\tilde{v}_p + \bar{v}_p)$. In both cases, the red and blue filled circles represent the median value of all the clusters in the RAMSES simulation and the GADGET-3 simulation respectively. The vertical lines are 1σ error bars.

3.5 Influence of the infall velocity: The mass excess

In this section, the influence that the infall velocity has on the cluster dynamics is estimated. From Figure 1 it is apparent that, according to the simulations, within ~ 1.3 and 2 virial radii respectively, there is a negative mean peculiar velocity in galaxy clusters. With equation (3.11) representing this infall velocity, I now have the tools needed to estimate the influence that the infall velocity has on the cluster dynamics and on the total cluster mass in particular. First though, for convenience, I introduce the new quantity

$$S(r) = \bar{v}_p \frac{\partial \bar{v}_p}{\partial r} + H_0 \left(\bar{v}_p + r \frac{\partial \bar{v}_p}{\partial r} \right), \quad (3.15)$$

where H_0 is the Hubble parameter at the present epoch (i.e. the Hubble constant). S was first presented in Falco et al. 2013. It is the extra term that has (re)appeared in Jeans equation and the Euler equation after including radial streaming motion, time dependence and the gravitational potential components due to the underlying cosmology of our universe, and it can be thought of as a correction to the standard Jeans equation and the equation of hydrostatic equilibrium. Note that I have completely ignored the term $\frac{\partial \bar{v}_p}{\partial t}$, for the simple reason that it is very difficult to estimate. I shortly discuss the consequence of doing this in section 3.8.2. Throughout the thesis, I refer to S as the "mass excess". By applying equation (3.11) to equation (3.15), S can be calculated analytically.

Figure 3 shows the mass excess of the two simulations normalized with respect to $GM(r)/r^2$, where $M(r)$ is the mass profile calculated from the density profiles extracted from the two simulations. In both cases, it is apparent that the influence of the infall velocity is negligible within $1 r_v$ (as stated earlier), while it has a non-negligible contribution between $1 r_v$ and $2 r_v$. In fact, according to the RAMSES plot it has a maximum contribution of $\sim 15\%$ at $\sim 1.78 r_v$ compared to the correct total mass of the cluster. A positive value of S means that the standard Jeans equation and the equation of hydrostatic equilibrium overestimate the total mass and vice versa. It is unfortunate that the GADGET-3 data only extends to $\sim 1.3 r_v$, since it is mainly outside this region that the influence becomes important. It is however, worth to note that within $1.3 r_v$, the GADGET-3 plot shows a similar behavior to the RAMSES plot⁸, and it even seems to predict an influence at lower radii than the RAMSES plot.

On the basis of Figure 3, I conclude that the correction to the standard Jeans equation and the equation of hydrostatic equilibrium (i.e. the infall velocity

⁸This is of course not so strange, since I have used the same function and parameters for the velocity profile in both simulations.

represented by the S term) becomes important (non-negligible) to the dynamics of galaxy clusters beyond the virial radius.

Figure 4 shows the contribution from each term in S relative to $GM(r)/r^2$. The term $\bar{v}_p \frac{\partial \bar{v}_p}{\partial r}$ gives the largest and the only positive contribution, while the terms $H_0 \bar{v}_p$ and $H_0 r \frac{\partial \bar{v}_p}{\partial r}$ give smaller (but non-negligible) and negative contributions.

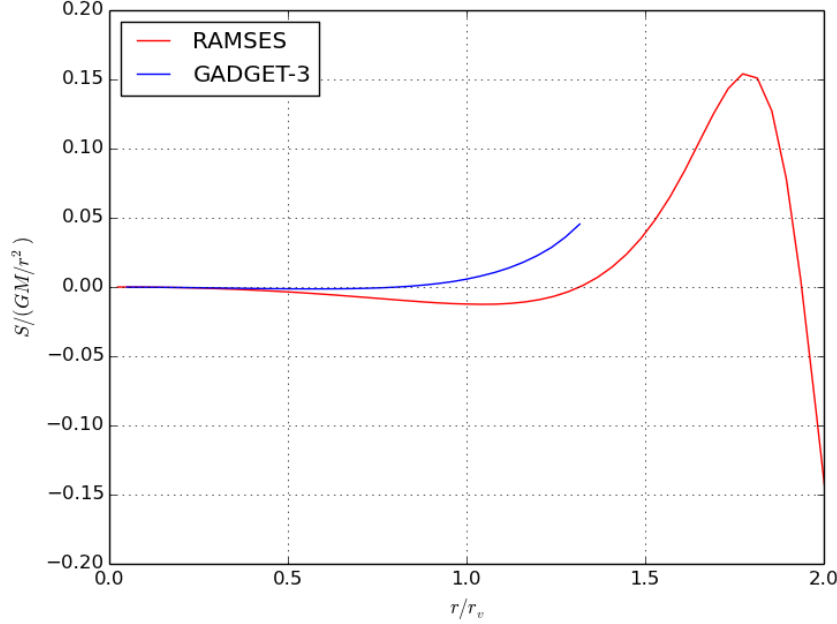


Figure 3: The mass excess, S , given by equation (3.15), relative to $GM(r)/r^2$, where $M(r)$ is the (correct) total mass profile calculated from the density profiles extracted from the numerical simulations. The red line represents the RAMSES simulation while the blue line represents the GADGET-3 simulation. The $GM(r)/r^2$ value used is the median value from the particular simulation. Furthermore, in order to get the correct unit (and value) on S , \bar{v}_p has been multiplied by the circular velocity at the virial radius, $v_v = \sqrt{GM_v/r_v}$, while $\partial \bar{v}_p / \partial r$ has been multiplied by v_v/r_v . Note that there are of course error bars to the median value of the mass excess, but these have been excluded from the figure in order to make it more legible.

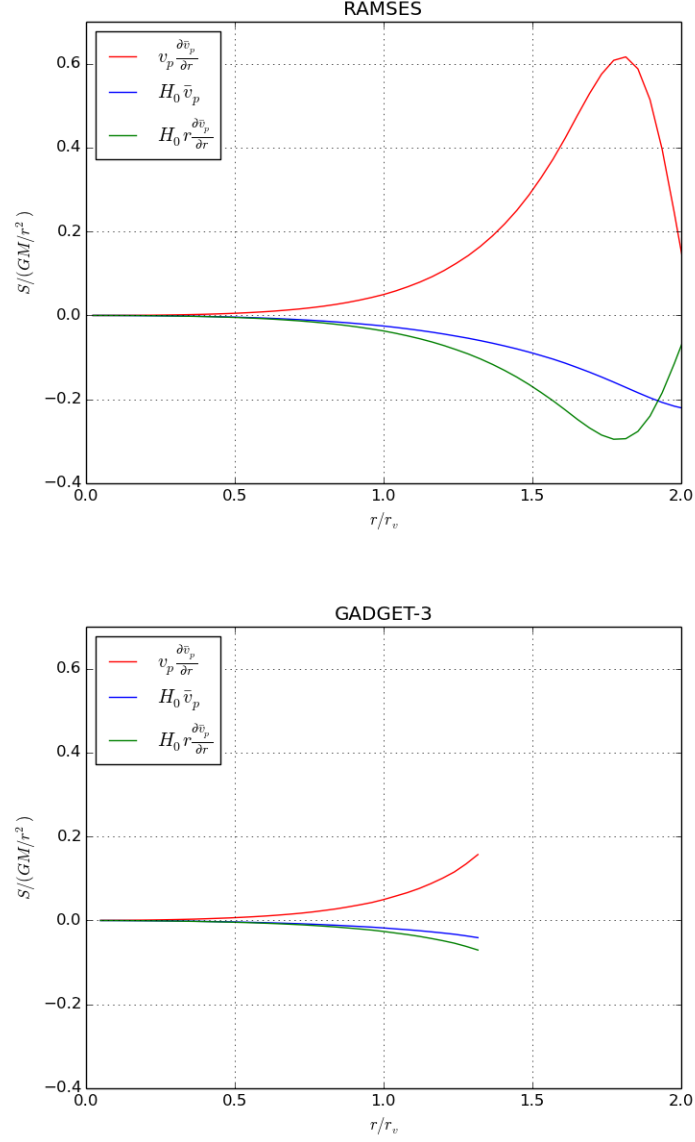


Figure 4: Each term that contributes to S given by equation (3.15) relative to $GM(r)/r^2$. The upper plot represents the RAMSES simulation, while the lower one represents the GADGET-3 simulation. In both cases, the red, blue and green lines represent the terms $\bar{v}_p \frac{\partial \bar{v}_p}{\partial r}$, $H_0 \bar{v}_p$ and $H_0 r \frac{\partial \bar{v}_p}{\partial r}$ respectively.

3.6 Measuring β

In this section, I solve the DM dynamics and provide a method for measuring the anisotropy parameter, β . The total mass profile of galaxy clusters can be calculated using either the generalized equation describing the gas part of cluster dynamics, i.e. equation (3.9) or the equation describing the dark matter part, i.e. equation (3.10). In order to do this, several parameter profiles (in addition to the radial velocity profile) need to be known: $T(r)$, $\rho(r)$ and $\bar{v}_r(r)$ or $\bar{v}_p(r)$ in equation (3.9) and $\sigma_r(r)$, $\nu(r)$, $\beta(r)$ and $\bar{v}_r(r)$ or $\bar{v}_p(r)$ in equation (3.10).

However, the only direct information we receive from cosmological structures is the radiation that they emit. This information is very valuable though, since some of the parameters can be estimated from it via theories. For example, it is relatively simple to calculate the density and temperature profiles of the baryonic matter from its observed emission profile as explained briefly below (in section 3.7), and since $\bar{v}_p(r)$ has already been parameterized, equation (3.9) (describing the gas) is "complete" in the sense that $M(r)$ is the only unknown variable. Therefore, if one observes the density and temperature profiles of the baryonic matter in a galaxy cluster and adopt \bar{v}_p as given by equation (3.11), then one can calculate a more exact cluster mass profile by using equation (3.9) than by using the equation of hydrostatic equilibrium given by equation (3.2).

Equation (3.10) (describing the dark matter) is more difficult to complete for the reason that dark matter does not emit any radiation, since this means that there are no directly observable DM parameters. Anyhow, it is possible to solve the DM dynamics, and I now present one particular way of doing this, which will result in two expressions for the anisotropy parameter, β .

I start by defining a DM temperature⁹ given by

$$T_{\text{DM}} \equiv \frac{\mu m_H}{k_B} \frac{1}{3} (\sigma_r^2 + \sigma_\theta^2 + \sigma_\phi^2). \quad (3.16)$$

This definition of the DM temperature was first presented in Hansen & Piffaretti 2007, and T_{DM} could be defined in other ways as well, as long as it has the right dimension. I return to this topic in section 3.8.3. The DM temperature can be related to the gas temperature by

$$T_{\text{DM}} = \kappa T_{\text{gas}}. \quad (3.17)$$

In general κ is a function of radius, and it can be estimated through numerical simulations (see section 3.6.1). Equations (3.16) and (3.17) make it possible

⁹The concept of a DM temperature is not well defined, since there is no thermodynamic equilibrium for a collisionless gas. The distribution functions are fairly close to having Maxwell-Boltzmann shape though (Hansen et al. 2006), so the concept is not completely unnatural.

to solve the DM dynamics using measurements of the gas, which will now be explained.

In this section, I only include the main equations, while a detailed derivation can be found in appendix G. Rewriting the generalized Jeans equation given by equation (3.10) and using equations (3.16) and (3.17) to get rid of β , I obtain a differential equation for the radial velocity dispersion given by

$$\sigma_r^2 \left(\frac{\partial \ln \nu}{\partial \ln r} + \frac{\partial \ln \sigma_r^2}{\partial \ln r} + 3 \right) = \psi(r, t), \quad (3.18)$$

where

$$\psi(r, t) = \frac{3k_B T_{\text{DM}}}{\mu m_H} - \frac{GM(r)}{r} - r\tilde{F}(r, t), \quad (3.19)$$

and

$$\tilde{F}(r, t) = \left(\tilde{v}_r \frac{\partial \tilde{v}_r}{\partial r} + \frac{\partial \tilde{v}_r}{\partial t} \right) + qH^2 r = \left(\tilde{v}_p \frac{\partial \tilde{v}_p}{\partial r} + H \left(\tilde{v}_p + r \frac{\partial \tilde{v}_p}{\partial r} \right) + \frac{\partial \tilde{v}_p}{\partial t} \right). \quad (3.20)$$

In the derivation of equation (3.18), I have assumed that the tangential velocity dispersions are equal, i.e. $\sigma_\theta = \sigma_\phi = \sigma_t$, which means that the anisotropy parameter is given by $\beta = 1 - \frac{\sigma_t^2}{\sigma_r^2}$. The error associated with this assumption has been shown to be negligibly small (see Bullock et al. 2001). The solution to equation (3.18) is

$$\sigma_r^2(r) = \frac{1}{\nu(r)r^3} \int_0^r \psi(r') \nu(r') r'^2 dr', \quad (3.21)$$

where the DM density, ν , can be determined by subtracting the gas density from the total density, which in turn can be determined from the total mass profile. With the radial velocity dispersion determined by equation (3.21), the only unknown DM parameter remaining is the anisotropy parameter, β , which can now be obtained in two ways. It can be recovered from equations (3.16) and (3.17), i.e. the relation between the DM temperature and the gas temperature, which yields

$$\beta = \frac{3}{2} \left(1 - \kappa \frac{k_B T_{\text{gas}}}{\mu m_H \sigma_r^2} \right). \quad (3.22)$$

Alternatively, β can be recovered directly from the generalized Jeans equation, since it is now as mentioned the only unknown parameter in the equation. This way I get

$$\beta = -\frac{1}{2} \left(\frac{\partial \ln \nu}{\partial \ln r} + \frac{\partial \ln \sigma_r^2}{\partial \ln r} + \frac{GM(r)}{r \sigma_r^2} + \frac{r}{\sigma_r^2} \tilde{F}(r, t) \right). \quad (3.23)$$

Ideally, equations (3.22) and (3.23) should of course yield the same β profile.

Knowledge of β can be used to put constraints on the collisionality of DM particles. If dark matter was collisional like baryonic matter, it would equilibrate through internal collisions, and in that case, $\beta = 0$. However, dark matter is known to be effectively collisionless on the dynamical timescale of galaxy clusters ($\tau \sim 10^9$ yr), and thus β has a non-zero radial dependence as seen in Figure 5. Anyhow, it is possible that dark matter does have a tiny collision rate, which can be estimated from the value of β . In Host et al. 2009, an order of magnitude upper limit to the scattering cross section of dark matter of $\lesssim 1 \text{ cm}^2/\text{g}$ is obtained.

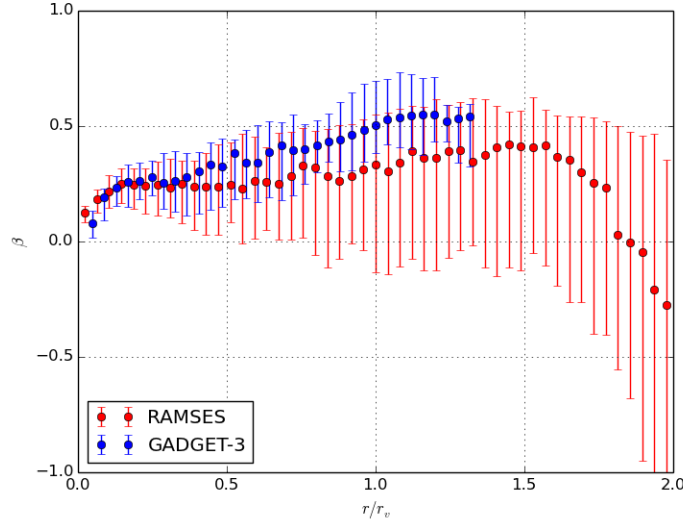


Figure 5: The anisotropy parameter, β , predicted by numerical simulations. In the simulations, the dark matter is assumed to be completely collisionless. The red and blue filled circles represent the median value of all the clusters in the RAMSES simulation and the GADGET-3 simulation respectively. The vertical lines are 1σ error bars.

3.6.1 Estimating the κ profile

In order for the DM dynamics model presented above to be complete, the radial κ profile also needs to be determined. I have estimated it using the data from the numerical simulations described in section 3.3.

Figure 6 shows the κ profile with the upper and lower plot representing the RAMSES and GADGET-3 simulation respectively. In both cases, the value of

κ lies relatively close (within a factor of 2) to 1 (corresponding to $T_{\text{DM}} = T_{\text{gas}}$) at all radii, but the two simulations predict different shapes and values for the profile. The profile resulting from the RAMSES simulation starts out at a value of ~ 0.5 and grows all the way out to $2r_v$, where it reaches a maximum value of ~ 1.5 , while the one resulting from the GADGET-3 simulation starts out at a value of ~ 1.3 , reaches its maximum value of ~ 2 at relatively low radius (within $0.5r_v$) and then decreases to a value of ~ 1.25 at $\sim 1.3r_v$, where the data stops. Rough ("chi-by-eye") fits (the red lines) have been added to the plots, where I have used $f(r/r_v) = ar^b$ ($a = 1.323$, $b = 0.215$) as the fitting function to the RAMSES plot, while $f(r/r_v) = ar^b - cr$ ($a = 3.7$, $b = 0.31$, $c = 2.15$) has been used as the fitting function to the GADGET-3 plot.

3.6.2 Incomplete modelling of the gas physics?

In Figure 7, I have plotted the temperature of both the gas and the dark matter, where the upper and lower plot represents the RAMSES and GADGET-3 simulation respectively. This figure makes the difference between the κ profiles of the two simulations apparent. The shapes of the DM temperature profiles of the simulations are similar (they both drop with a factor of between 1.5 and 2 from the innermost region to one virial radius), but there is a noticeable difference between the shapes of the gas temperature profiles. The RAMSES gas temperature drops with a factor of ~ 4.5 from the innermost region to one virial radius (from $\sim 6.5 \cdot 10^7 \text{K}$ to $\sim 1.4 \cdot 10^7 \text{K}$), while the GADGET-3 gas temperature drops with a factor of ~ 1.7 in the same region (from $\sim 1.2 \cdot 10^8 \text{K}$ to $\sim 7 \cdot 10^7 \text{K}$).

The difference between the gas temperature profiles of the two simulations induces a corresponding difference in the κ profile (since the DM temperature profiles are almost equivalent), and thus the DM parameters depending on κ (T_{DM} , σ_r and β) of course, in turn, depend on which simulation one uses for the parameterization of κ (which it ideally should not). The difference between the gas temperature profiles is probably caused by diverse modelling of e.g. gas cooling, SN feedback or AGN feedback, and in that case, the implementation of the gas physics is insufficient in at least one of the simulations.¹⁰ This is exactly the reason why we have used two different simulations. We cannot know which

¹⁰One should have in mind that the clusters extracted from the two simulations have different total mass (most of the clusters from the GADGET-3 simulation have a total mass greater than 10^{15}M_{\odot} , while this only applies to one of the clusters from the RAMSES simulation). It is unlikely though, that this difference causes the relatively large difference between the shapes of the gas temperature profiles, since the dynamics and timescales applying to 10^{14}M_{\odot} and 10^{15}M_{\odot} clusters are essentially the same.

of the simulations used in this project is right (if any), but we do know that something is not right. Therefore, more time must be devoted to the prospect of determining κ , and the next step could be that we were given direct access to unprocessed simulation data. That way, we would have more control over the data, and it would for example be easier to check for errors.

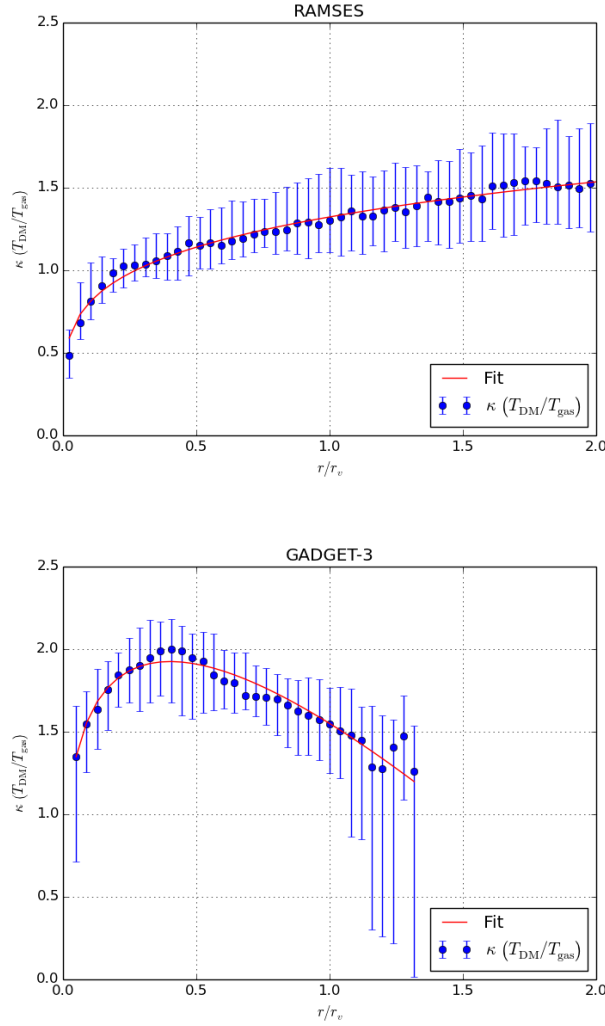


Figure 6: The relation between the DM temperature and the gas temperature, $\kappa = T_{\text{DM}}/T_{\text{gas}}$, as a function of radius. The upper plot represents the RAMSES simulation, while the lower one represents the GADGET-3 simulation. In both cases, the blue filled circles represent the median value of κ for the entire cluster samples, while the vertical lines are 1σ error bars. The red curves are rough "chi-by-eye" fits.

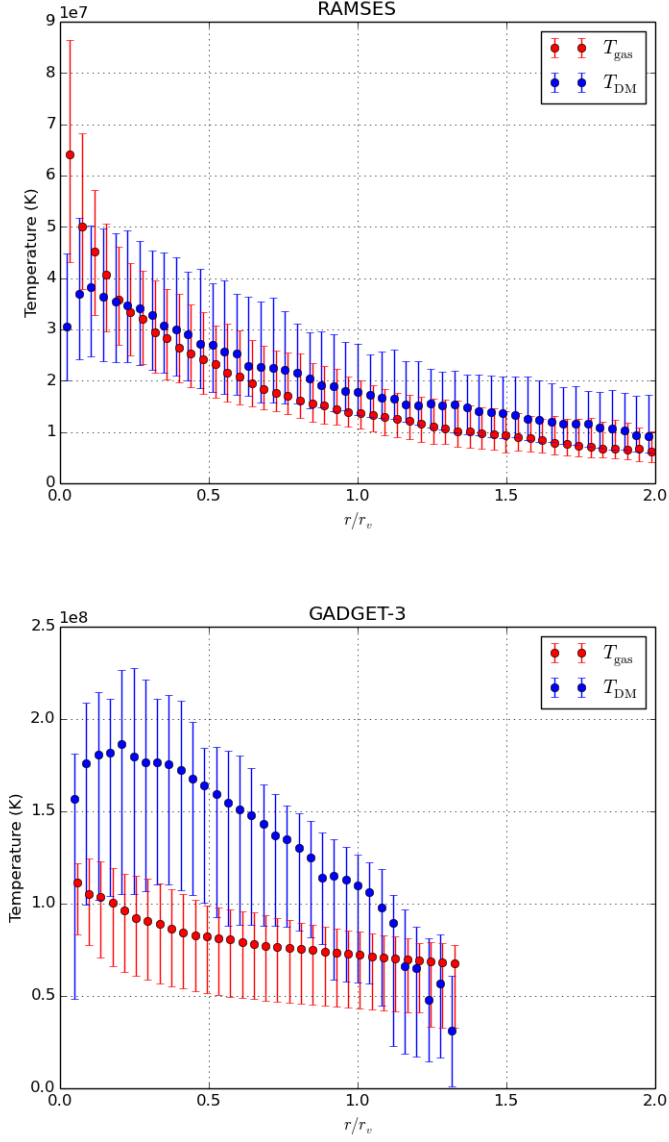


Figure 7: Temperature in units of Kelvin (K) as a function of radius. The upper plot represents the RAMSES simulation, while the lower one represents the GADGET-3 simulation. In both cases, the red and blue filled circles represent the median value of the gas temperature and the DM temperature respectively. The vertical lines are 1σ error bars. Note that the gas part has been displaced slightly to the right in both plots for visual purposes.

3.7 Extracting the gas density and temperature from observations

3.7.1 X-ray observations

Now, all the theory is in place, and the DM dynamics model presented above is ready to process data from observations of real galaxy clusters. As previously mentioned, radiation is the only source of information that we receive from galaxy clusters, and the main part of the radiation coming from the hot ICM is X-ray radiation. An extensive description of X-ray emission mechanisms in galaxy clusters can be found in Sarazin 1986, as I will here only provide a brief description.

The density and temperature of the ICM can be extracted from an observed X-ray spectrum of the particular galaxy cluster. This job is usually done by specialists, who then give other physicists access to their data. Figure 8 shows an X-ray spectrum of the Virgo Cluster (the closest galaxy cluster to the Local Group). The continuum part of the spectrum is primarily caused by thermal bremsstrahlung (free-free emission) with contributions from recombination (free-bound) emission and two-photon decay (bound-bound emission). Bremsstrahlung is radiation produced by the acceleration of a charged particle (usually an electron) when deflected by another charged particle (usually an ion). When deflected, the moving particle loses kinetic energy, which is emitted in the form of a photon. At the temperature of the ICM, hydrogen and helium is virtually fully ionized, and most of the bremsstrahlung results from encounters between free electrons and ions from these elements.

It is evident from Figure 8 that, in addition to the continuum, emission lines (from e.g. magnesium, oxygen and iron) are also present in the X-ray spectrum of the Virgo Cluster - this is a general feature of X-ray spectra from galaxy clusters. Emission lines result from excited ions decaying to a lower energy level while emitting a photon of characteristic energy depending on the specific ion.

The combination of the different emission processes mentioned above results in an X-ray spectrum similar to the one seen in Figure 8. The bremsstrahlung emission per unit time per unit volume per unit frequency range, ϵ , scales as (Rybicki & Lightman 1979) $T^{-1/2} \exp(-E/k_B T) \bar{g}_{ff}(E, T)$, where $\bar{g}_{ff}(E, T)$ is the so called Gaunt factor averaged over velocity. Since ϵ depends on parameters depending on energy and temperature exclusively, ϵ depends on energy and temperature only as well, and with ϵ given as function of energy by the X-ray spectrum, the temperature can be determined directly from a fit to the spectrum.

Meanwhile, the density of the gas can be determined from the height of the

X-ray spectrum. A higher density results in more free ions and electrons, which in turn results in more bremsstrahlung and therefore a higher emission rate. In particular, the height of the spectrum is proportional to the density squared.

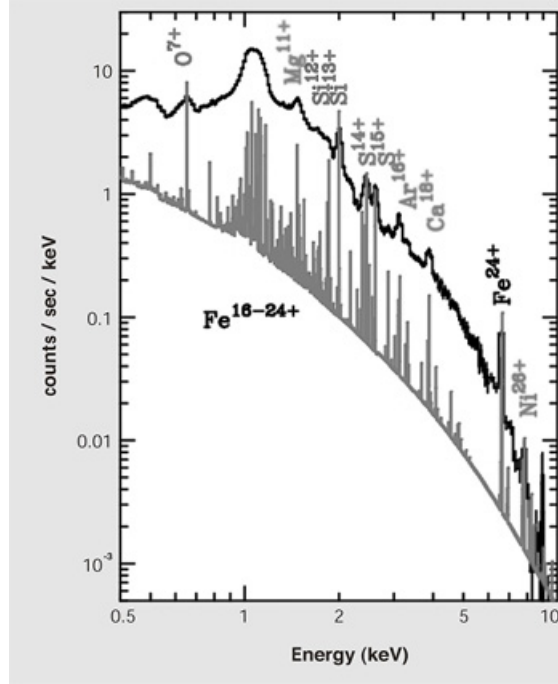


Figure 8: X-ray spectrum of the Virgo Cluster. The spectrum shows the distribution of the number of X-ray photons (from which the "amount" of emission can be obtained) as a function of energy. The upper line is the raw unprocessed spectrum, while the lower line is the "true" spectrum emitted by the ICM, where the influence of the detector has been accounted for. The figure is from <http://www.isas.jaxa.jp/e/forefront/2004/matsushita/02.shtml>.

3.7.2 Deprojection ("onion peeling")

The optical depth of the ICM is very low, which means that almost all radiation travels unaffected through a galaxy cluster (Sarazin 1986). Therefore, the X-ray emission from a galaxy cluster, observed along a given line of sight, results in a spectrum with the emission coming from all of the gas in the cluster lying along that particular line of sight. What one wants however, is the emission received from a particular gas shell (or bin), which will allow one to determine the

temperature in each shell (where it is assumed to be constant). In order to account for this, one has to deproject the "two-dimensional" spectrum to recover the correct three-dimensional properties of the cluster. The outermost shell of a galaxy cluster does not need to be modified, since when observing the "edge" of the cluster, no gas from inner shells can "obscure" the data as illustrated by Figure 9. When the emission spectrum from the outermost shell has been determined, one can determine the spectrum from the second outermost shell. When observing the emission from this shell however, one cannot avoid observing emission coming from the outermost one as well, so the emission from the outermost shell has to be subtracted subsequently. The process, which is sometimes analogously referred to as onion peeling, continues in this way until the emission spectrum resulting from the central region has been obtained. One particular deprojection package can be found at <http://cxc.harvard.edu/contrib/deproject/>.

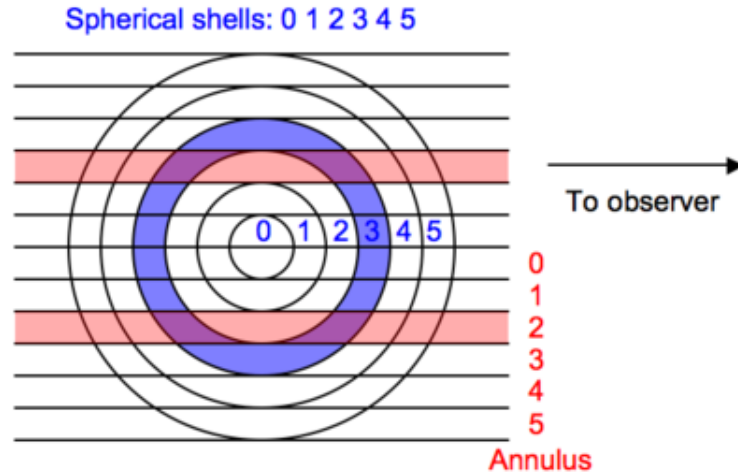


Figure 9: Illustration of the deprojection process. When one observes along annulus 5, the received emission comes from shell 5 only. However, when one observes along e.g. annulus 2, shell 2, 3, 4 and 5 all contribute to the received emission. Therefore, in order to determine the amount of emission coming exclusively from shell 2, one has to subtract the contributions from shell 3, 4 and 5. The figure is from <http://cxc.harvard.edu/contrib/deproject/>.

3.8 Discussion

3.8.1 The numerical simulations

The numerical simulations used in this project have been run with completely different codes, and thus the chances of avoiding (or detecting) systematic errors should be optimal. It is unfortunate though, that the GADGET-3 data only extends to $\sim 1.3 r_v$, since it is mainly outside this radius that the work done in this project is relevant. Therefore, it would be desirable to compare the results to data from other numerical simulations. Hopefully, this would improve the results and conclusions of this thesis.

3.8.2 The mass excess

In section 3.5, the mass excess, S , is given as a function of radius only:

$$S(r) = \bar{v}_p \frac{\partial \bar{v}_p}{\partial r} + H_0 \left(\bar{v}_p + r \frac{\partial \bar{v}_p}{\partial r} \right). \quad (3.24)$$

This is just an approximation to the true mass excess given by

$$S(r, t) = \bar{v}_p \frac{\partial \bar{v}_p}{\partial r} + H(t) \left(\bar{v}_p + r \frac{\partial \bar{v}_p}{\partial r} \right) + \frac{\partial \bar{v}_p}{\partial t}, \quad (3.25)$$

which also depends on time. In equation (3.24), the term $\frac{\partial \bar{v}_p}{\partial t}$ has been ignored, while the Hubble parameter, $H(t)$, has been replaced by the Hubble constant, H_0 , for the equation to yield a "snapshot" of the current epoch. Ideally, the ∂_t term should be included when calculating the mass excess, but it is rather circumstantial to estimate, which is the sole reason why it has been ignored. An effort to estimate its value has been made in Falco et al. 2013, but the result was not completely conclusive and has therefore not been adopted in this thesis.

3.8.3 The dark matter temperature

In section 3.6, I defined the DM temperature as

$$T_{\text{DM}} \equiv \frac{\mu m_H}{k_B} \frac{1}{3} (\sigma_r^2 + \sigma_\theta^2 + \sigma_\phi^2). \quad (3.26)$$

Another equally correct definition could be

$$\tilde{T}_{\text{DM}} \equiv \frac{\mu m_H}{k_B} (\sigma_r^2 \sigma_\theta^2 \sigma_\phi^2)^{1/3}, \quad (3.27)$$

since it has the same dimension as equation (3.26), and there are of course more possibilities.

Figure 10 shows the difference between the two definitions of the dark matter temperature given by equations (3.26) and (3.27) for both the RAMSES simulation (red) and the GADGET-3 simulation (blue). In both cases, $T_{\text{DM}}/\tilde{T}_{\text{DM}} \approx 1$ at all radii, which implies that $T_{\text{DM}} \approx \tilde{T}_{\text{DM}}$ at all radii.

Figure 11 shows the $\tilde{\kappa}$ profile, where the tilde denotes that the alternative definition given by equation (3.27) has been used for the DM temperature. Comparing Figure 11 to Figure 6 (section 3.6.1) makes it apparent that the $\tilde{\kappa}$ profile is essentially identical to the κ profile for the respective simulations. This indicates that whether one chooses to define the DM temperature by equation (3.26) or by equation (3.27) has no significant influence on the κ profile. Note however, that using \tilde{T}_{DM} instead of T_{DM} will alter the first expression for β in section 3.6 (equation (3.22)), but the method for obtaining the altered expression is the same. Furthermore, the obtained β profile should be the same regardless of the DM temperature definition used.

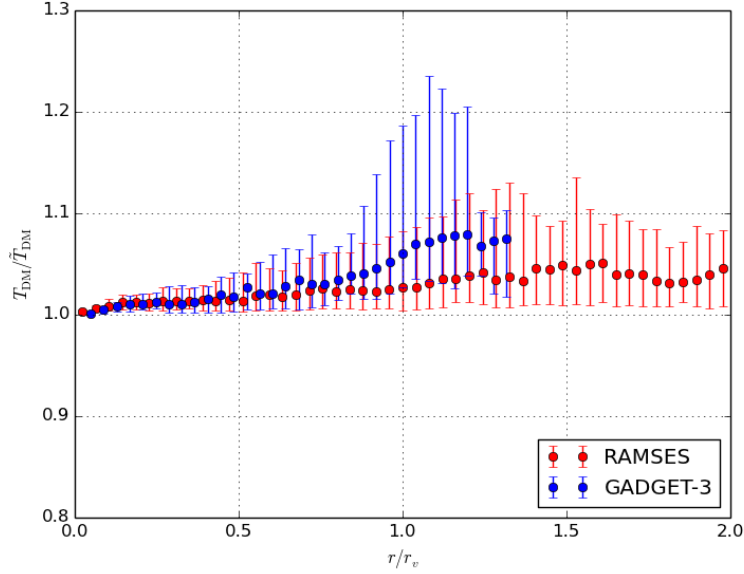


Figure 10: Difference between T_{DM} given by equation (3.26) and \tilde{T}_{DM} given by equation (3.27). In particular, $T_{\text{DM}}/\tilde{T}_{\text{DM}}$ is plotted as a function of radius. The red and blue filled circles represent the median value of all the clusters in the RAMSES simulation and the GADGET-3 simulation respectively. The vertical lines are 1σ error bars.

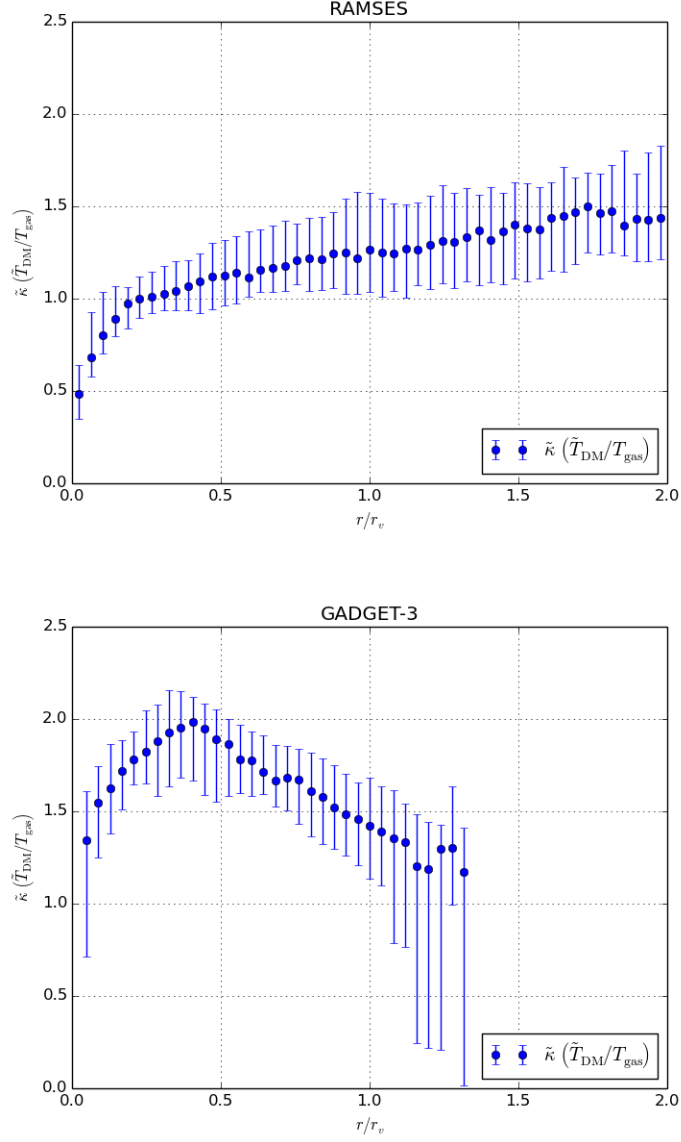


Figure 11: The relation between the alternative DM temperature defined by equation (3.27) and the gas temperature, $\tilde{\kappa} = \tilde{T}_{\text{DM}}/T_{\text{gas}}$, as a function of radius. The upper plot represents the RAMSES simulation, while the lower one represents the GADGET-3 simulation. In both cases, the blue filled circles represent the median value of $\tilde{\kappa}$ for the entire cluster samples, while the vertical lines are 1σ error bars.

3.9 Summary and conclusion

The main purpose of this part of the thesis (part 2) was to estimate the influence that the infall velocity in galaxy clusters has on the cluster dynamics and on the total mass profile of clusters in particular. This has been done on the basis of the Euler equation and the collisionless Boltzmann equation given by equations (3.1) and (3.3) respectively, and using data from the numerical simulations introduced in section 3.3. I found that within one virial radius, the infall velocity has effectively no influence, i.e. in this region, galaxy clusters are virtually fully equilibrated, and thus the assumption of hydrostatic equilibrium is justifiable. However, between one and two virial radii, the infall velocity does have a non-negligible influence on the cluster dynamics. In this region, according to the simulations, the standard Jeans equation and the equation of hydrostatic equilibrium given by equations (3.2) and (3.6) respectively, in general overestimate the total mass. According to the RAMSES simulation, the largest effect is at ~ 1.78 times the virial radius, where the standard equations overestimate the total cluster mass by $\sim 15\%$ (see Figure 3). A more accurate mass profile is given by the generalized equations describing the dynamics of galaxy clusters (equations (3.9) and (3.10)).

While investigating the infall velocity in galaxy clusters, I found that the infall velocity of the baryonic matter and that of the dark matter seem to be effectively equal at all radii as shown in Figure 1 and Figure 2. That this is the case is not quite trivial, since baryonic particles and DM particles give off energy differently (by collisional and non-collisional effects respectively).

In section 3.6, I have used equation (3.9) and equation (3.10) to solve the dark matter dynamics of galaxy clusters, and two ways of measuring the anisotropy parameter, β , are presented (equations (3.22) and (3.23)). In order to apply this in practice, the density and temperature profiles of the gas (ICM) need to be known, and in section 3.7, I have provided a brief description of how these can be obtained.

4 References

- Barnes L. A., Francis M. J., James J. B., Lewis G. F., 2006, *Joining the Hubble Flow: implications for expanding space*, MNRAS 373 382 [astro-ph/0609271]
- Binney J., Tremaine S., 2008, *Galactic Dynamics* (Second Edition), Princeton University Press
- Bonafede A., Dolag K., Stasyszyn F., Murante G., Borgani S., 2011, *A non-ideal MHD Gadget: Simulating massive galaxy clusters*, MNRAS, 418, 2234
- Bullock J. S., Dekel A., Kolatt T. S., Kravtsov A. V., Klypin A. A., Porciani C., Primack J. R., 2001, *A Universal Angular Momentum Profile for Galactic Halos*, ApJ, 555, 240
- Cuesta A. J., Prada F., Klypin A. A., Moles M., 2008, *The virialized mass of dark matter haloes*, MNRAS, 389, 385
- Falco M., Mamon G. A., Wojtak R., Hansen S. H., Gottlöber S., 2013, *Dynamical signatures of infall around galaxy clusters: a generalized Jeans equation*, MNRAS, 436, 2639
- Grøn Ø., Elgarøy Ø., 2007, *Is space expanding in the Friedmann universe models?*, Am. J. Phys. 75, 151
- Hansen S. H., Moore B., Zemp M., Stadel J., 2006, *A universal velocity distribution of relaxed collisionless structures*, Journal of Cosmology and Astro-Particle Physics, 1, 14
- Hansen S. H., Piffaretti R., 2007, *Measuring the dark matter velocity anisotropy in galaxy clusters*, A&A, 476, L37
- Herman R. L., 2008, *Derivation of the Geodesic Equation and Defining the Christoffel Symbols*, <http://people.uncw.edu/>
- Host O., Hansen S. H., Piffaretti R., Morandi A., Ettori S., Kay S. T., Valdarnini R., 2009, *Measurement of the Dark Matter Velocity Anisotropy in Galaxy Clusters*, Astrophys. J. 690, 358
- Martizzi D., Mohammed I., Teyssier R., Moore B., 2014, *The biasing of baryons on the cluster mass function and cosmological parameter estimation*, MNRAS, 440, 2290
- Peebles P. J. E., 1980, *Princeton Series in Physics: The Large-Scale Structure of the Universe*, Princeton University Press
- Planelles S., Borgani S., Fabjan D., Killedar M., Murante G., Granato G. L., Ragone-Figueroa C., Dolag K., 2014, *On the role of AGN feedback on the thermal and chemodynamical properties of the hot intracluster medium*, MNRAS, 438, 195

- Rybicki G. B., Lightman A. B., 1979, *Radiative Processes in Astrophysics*, New York
- Ryden B., 2003, *Introduction to cosmology*, Addison Wesley
- Sarazin C. L., 1986, *X-ray emission from clusters of galaxies*, Reviews of Modern Physics, 58, 1
- Springel V., 2005, *The cosmological simulation code GADGET-2*, MNRAS, 364, 1105
- Teyssier R., 2002, *Cosmological hydrodynamics with adaptive mesh refinement. A new high resolution code called RAMSES*, AAP, 385, 337–364

Appendix

A

In this appendix, a derivation of equation (2.22) and equation (2.23) is provided. The Christoffel symbol is given by equation (2.19), and as mentioned in section 2.5, the only non-vanishing Christoffel symbols are $\Gamma_{\chi t}^\chi$, $\Gamma_{t\chi}^\chi$ and $\Gamma_{\chi\chi}^t$. By symmetry I have that $\Gamma_{\chi t}^\chi = \Gamma_{t\chi}^\chi$, so

$$\Gamma_{\chi t}^\chi = \Gamma_{t\chi}^\chi = \frac{1}{2}g^{\chi\chi} \left[\frac{\partial g_{\chi\chi}}{\partial t} + \frac{\partial g_{\chi\chi}}{\partial \chi} - \frac{\partial g_{t\chi}}{\partial \chi} \right] = \frac{1}{2}a^{-2} \left(\frac{\partial a^2}{\partial t} + \frac{\partial a^2}{\partial \chi} \right) = \frac{1}{2a^2} \frac{\partial a^2}{\partial t},$$

where

$$\begin{aligned} \frac{\partial a^2}{\partial t} &= a \frac{\partial a}{\partial t} + a \frac{\partial a}{\partial t} = 2a \frac{\partial a}{\partial t} = 2a\dot{a} \quad => \\ \Gamma_{\chi t}^\chi &= \Gamma_{t\chi}^\chi = \frac{1}{2a^2} 2a\dot{a} = \frac{\dot{a}}{a}. \end{aligned} \quad (\text{A.1})$$

This is the first (left) part of equation (2.22). Meanwhile, the last non-vanishing Christoffel symbol yields

$$\Gamma_{\chi\chi}^t = \frac{1}{2}g^{tt} \left[\frac{\partial g_{\chi t}}{\partial t} + \frac{\partial g_{t\chi}}{\partial t} - \frac{\partial g_{\chi\chi}}{\partial t} \right] = -\frac{1}{2c^2} \left(-\frac{\partial a^2}{\partial t} \right) = \frac{1}{2c^2} 2a\dot{a} = \frac{a\dot{a}}{c^2}. \quad (\text{A.2})$$

This is the second (right) part of equation (2.22).

For the sake of completeness, the remaining (vanishing) Christoffel symbols have also been calculated. Since I am dealing with radial particle motion exclusively, all symbols involving θ and ϕ vanish, and furthermore, since $g_{\mu\nu}$ is a diagonal matrix, I only get a contribution, when $\rho = \mu$. Thus, the remaining symbols (not yet calculated) are:

$$\begin{aligned} \Gamma_{\chi\chi}^\chi &= \frac{1}{2}g^{\chi\chi} \left[\frac{\partial g_{\chi\chi}}{\partial \chi} + \frac{\partial g_{\chi\chi}}{\partial \chi} - \frac{\partial g_{\chi\chi}}{\partial \chi} \right] = \frac{1}{2}a^{-2} \frac{\partial a^2}{\partial \chi} = 0, \\ \Gamma_{tt}^\chi &= \frac{1}{2}g^{\chi\chi} \left[\frac{\partial g_{t\rho}}{\partial t} + \frac{\partial g_{\chi t}}{\partial t} - \frac{\partial g_{tt}}{\partial \chi} \right] = \frac{1}{2}a^{-2} \frac{\partial c^2}{\partial \chi} = 0, \\ \Gamma_{tt}^t &= \frac{1}{2}g^{tt} \left[\frac{\partial g_{tt}}{\partial t} + \frac{\partial g_{tt}}{\partial t} - \frac{\partial g_{tt}}{\partial t} \right] = \frac{1}{2}c^{-2} \frac{\partial c^2}{\partial t} = 0, \\ \Gamma_{\chi t}^t &= \Gamma_{t\chi}^t = \frac{1}{2}g^{tt} \left[\frac{\partial g_{tt}}{\partial \chi} + \frac{\partial g_{t\chi}}{\partial t} - \frac{\partial g_{\chi t}}{\partial t} \right] = \frac{1}{2}c^{-2} \frac{\partial c^2}{\partial t} = 0, \end{aligned} \quad (\text{A.3})$$

and as stated, they all vanish.

Now to equation (2.23). Substituting equation (A.1) into the geodesic equation given by equation (2.18) yields

$$\begin{aligned}
\frac{d^2\chi}{d\tau^2} + (\Gamma_{\chi t}^\chi + \Gamma_{t\chi}^\chi) \frac{d\chi}{d\tau} \frac{dt}{d\tau} &= \frac{d^2\chi}{d\tau^2} + 2 \frac{\dot{a}}{a} \frac{d\chi}{d\tau} \frac{dt}{d\tau} = 0 \quad \Rightarrow \\
\frac{d^2\chi}{d\tau^2} &= -2 \frac{\dot{a}}{a} \frac{d\chi}{d\tau} \frac{dt}{d\tau} = -2 \frac{\dot{a}}{a} \frac{d\chi}{dt} \frac{dt}{d\tau} \frac{dt}{d\tau} = -2 \frac{\dot{a}}{a} \frac{d\chi}{dt} \left(\frac{dt}{d\tau} \right)^2 = -2 \frac{\dot{a}}{a} \dot{\chi} \left(\frac{dt}{d\tau} \right)^2, \\
\left(\frac{dt}{d\tau} \right)^2 &= \left(\frac{d\tau}{dt} \right)^{-2} = \dot{\tau}^{-2} = \frac{1}{\dot{\tau}^2} \quad \Rightarrow \\
\frac{d^2\chi}{d\tau^2} &= -2 \frac{\dot{a}}{a} \frac{\dot{\chi}}{\dot{\tau}^2}. \tag{A.4}
\end{aligned}$$

This is the first (left) part of equation (2.23). Substituting equation (A.2) into the geodesic equation yields

$$\begin{aligned}
\frac{d^2t}{d\tau^2} + \Gamma_{\chi\chi}^t \frac{d\chi}{d\tau} \frac{d\chi}{d\tau} &= \frac{d^2t}{d\tau^2} + \frac{a\dot{a}}{c^2} \left(\frac{d\chi}{d\tau} \right)^2 = 0 \quad \Rightarrow \\
\frac{d^2t}{d\tau^2} &= -\frac{a\dot{a}}{c^2} \left(\frac{d\chi}{d\tau} \right)^2, \\
\frac{d\chi}{d\tau} &= \frac{d\chi}{dt} \frac{dt}{d\tau} = \frac{\dot{\chi}}{\dot{\tau}} \quad \Rightarrow \\
\frac{d^2t}{d\tau^2} &= -\frac{a\dot{a}}{c^2} \frac{\dot{\chi}^2}{\dot{\tau}^2}. \tag{A.5}
\end{aligned}$$

This is the second (right) part of equation (2.23).

B

In this appendix, a derivation of equation (2.24) is provided. During the derivation, I make use of the chain rule and the relation

$$\frac{d}{dx} \left(\frac{u}{v} \right) = \frac{v(du/dx) - u(dv/dx)}{v^2}.$$

$$\begin{aligned}
\ddot{\chi} &= \frac{d\dot{\chi}}{dt} = \frac{d}{dt} \left(\frac{d\chi}{dt} \right) = \frac{d}{dt} \left(\frac{d\chi/d\tau}{dt/d\tau} \right) \\
&= \left(\frac{dt}{d\tau} \cdot \frac{d}{dt} \left(\frac{d\chi}{d\tau} \right) - \frac{d\chi}{d\tau} \cdot \frac{d}{dt} \left(\frac{dt}{d\tau} \right) \right) \cdot \left(\frac{dt}{d\tau} \right)^{-2},
\end{aligned}$$

$$\begin{aligned}
\frac{d}{dt} \left(\frac{d\chi}{d\tau} \right) &= \frac{d}{d\tau} \left(\frac{d\chi}{d\tau} \right) \frac{d\tau}{dt} = \frac{d^2\chi}{d\tau^2} \frac{d\tau}{dt}, \\
\frac{d}{dt} \left(\frac{dt}{d\tau} \right) &= \frac{d}{d\tau} \left(\frac{dt}{d\tau} \right) \frac{d\tau}{dt} = \frac{d^2t}{d\tau^2} \frac{d\tau}{dt} \quad \Rightarrow \\
\ddot{\chi} &= \left(\frac{dt}{d\tau} \frac{d^2\chi}{d\tau^2} \frac{d\tau}{dt} - \frac{d\chi}{d\tau} \frac{d^2t}{d\tau^2} \frac{d\tau}{dt} \right) \left(\frac{dt}{d\tau} \right)^{-2} \\
&= \left(\frac{d\tau}{dt} \right)^2 \left(\frac{d^2\chi}{d\tau^2} - \frac{d\chi}{dt} \frac{d^2t}{d\tau^2} \right) \\
&= \dot{\tau}^2 \left(\frac{d^2\chi}{d\tau^2} - \dot{\chi} \frac{d^2t}{d\tau^2} \right). \tag{B.1}
\end{aligned}$$

Equation (B.1) is identical to equation (2.24).

C

In this appendix, a derivation of equation (2.26) is provided. I want to obtain equation (2.25) in terms of the dimensionless variable $y = c^2/\dot{\chi}^2$ instead of χ . In terms of y , I have $\dot{\chi} = c/\sqrt{y}$ and $\ddot{\chi} = c \frac{d}{dt} \left(\frac{1}{\sqrt{y}} \right) = -\frac{c\dot{y}}{2y^{3/2}}$, so equation (2.25) becomes

$$\begin{aligned}
-\frac{c\dot{y}}{2y^{3/2}} &= \frac{a\dot{a}}{c^2} \left(\frac{c}{\sqrt{y}} \right)^3 - 2\frac{\dot{a}}{a} \frac{c}{\sqrt{y}} = a\dot{a} \frac{c}{y^{3/2}} - 2\frac{\dot{a}}{a} \frac{c}{\sqrt{y}} \quad \Rightarrow \\
-\frac{1}{2}\dot{y}y^{-3/2} &= a\dot{a}y^{-3/2} - 2\frac{\dot{a}}{a}y^{-1/2} \quad \Rightarrow \\
-\frac{1}{2}\dot{y} &= a\dot{a} - 2\frac{\dot{a}}{a}y \quad \Rightarrow \\
\dot{y} &= 4\frac{\dot{a}}{a}y - 2a\dot{a}, \\
4\frac{\dot{a}}{a} &= \frac{d}{dt}(\ln a^4), \\
2a\dot{a} &= \frac{da^2}{dt} \quad \Rightarrow \\
\dot{y} &= y \frac{d}{dt}(\ln a^4) - \frac{da^2}{dt} \quad \Rightarrow \\
\dot{y} - y \frac{d}{dt}(\ln a^4) &= -\frac{da^2}{dt} \tag{C.1}
\end{aligned}$$

Equation (C.1) is identical to equation (2.26).

D

In this appendix, a derivation of the geodesic equation given by equation (2.18) is provided on the basis of Herman 2008. A geodesic is the curved-space generalization of the notion of a straight line, and the geodesic equation describes the motion of a particle in the four-dimensional spacetime.

In Euclidean space, the shortest path between two points is a straight line, and according to Newtonian physics, a free particle subject to no acceleration always follows a straight line through space (assuming it has an initial velocity greater than zero).

In general relativity, the theory of gravitation is described as "the presence of matter curves the four-dimensional spacetime" (and not as a force as in Newtonian physics). Therefore, in the presence of matter, spacetime is curved, and thus there may not exist any straight lines for free particles to follow. Instead, they move along a geodesic. For example, the orbit of the Earth around the Sun is a geodesic, and when an apple falls off a tree, that too follows a geodesic (if one disregards the friction from the atmosphere).

Note that if no matter is present, spacetime is flat, and thus a free particle will move along a straight line. Therefore, the geodesic equation has to reduce to the equation of a straight line, when no matter is present.

Derivation

In geometry, a line element ds can be expressed as

$$ds^2 = g_{\alpha\beta} dx^\alpha dx^\beta. \quad (\text{D.1})$$

Meanwhile, in GR, the path length, S , is given by

$$S = \int ds = \int \sqrt{g_{\alpha\beta} dx^\alpha dx^\beta}. \quad (\text{D.2})$$

I now consider the parameterized world line $x^\alpha = x^\alpha(\lambda)$ and multiply the RHS of equation (D.2) by $d\lambda/d\lambda$:

$$S = \int \left(g_{\alpha\beta} \frac{dx^\alpha}{d\lambda} \frac{dx^\beta}{d\lambda} \right)^{1/2} d\lambda. \quad (\text{D.3})$$

I want to minimize S , and this can be done using the Euler-Lagrange (E-L) equations, which for the parameter λ are given by

$$\frac{d}{d\lambda} \left(\frac{\partial L}{\partial(dx^\gamma/d\lambda)} \right) - \frac{\partial L}{\partial x^\gamma} = 0, \quad (\text{D.4})$$

where L is the Lagrangian given by

$$L = \frac{ds}{d\lambda} = \frac{\sqrt{g_{\alpha\beta} dx^\alpha dx^\beta}}{d\lambda} = \sqrt{g_{\alpha\beta} \frac{dx^\alpha}{d\lambda} \frac{dx^\beta}{d\lambda}}. \quad (\text{D.5})$$

I can get rid of the square root after the last equality sign by using $L' = L^2 = g_{\alpha\beta} \frac{dx^\alpha}{d\lambda} \frac{dx^\beta}{d\lambda}$ as the Lagrangian instead of L . This way I have

$$\frac{\partial L'}{\partial x} = \frac{\partial}{\partial x}(L^2) = L \frac{\partial L}{\partial x} + L \frac{\partial L}{\partial x} = 2L \frac{\partial L}{\partial x}, \quad (\text{D.6})$$

so equation (D.4) becomes

$$\frac{d}{d\lambda} \left(\frac{\partial L'}{\partial(dx^\gamma/d\lambda)} \right) - \frac{\partial L'}{\partial x^\gamma} = \frac{d}{d\lambda} \left(2L \frac{\partial L}{\partial(dx^\gamma/d\lambda)} \right) - 2L \frac{\partial L}{\partial x^\gamma} = 0,$$

and if λ satisfies that $L = \frac{ds}{d\lambda}$ is a constant, I have that

$$\begin{aligned} \frac{d}{d\lambda} \left(\frac{\partial L'}{\partial(dx^\gamma/d\lambda)} \right) - \frac{\partial L'}{\partial x^\gamma} &= 2L \frac{d}{d\lambda} \left(\frac{\partial L}{\partial(dx^\gamma/d\lambda)} \right) - 2L \frac{\partial L}{\partial x^\gamma} \\ &= 2L \left[\frac{d}{d\lambda} \left(\frac{\partial L}{\partial(dx^\gamma/d\lambda)} \right) - \frac{\partial L}{\partial x^\gamma} \right] = 0 \quad \Rightarrow \\ \frac{d}{d\lambda} \left(\frac{\partial L}{\partial(dx^\gamma/d\lambda)} \right) - \frac{\partial L}{\partial x^\gamma} &= 0. \end{aligned} \quad (\text{D.7})$$

So using L' as the Lagrangian leads to the same E-L equations as using L does, provided that λ is chosen so $\frac{ds}{d\lambda}$ is constant, i.e. λ has to be an affine parameter.

Now I want to rewrite equation (D.7) starting with the first term:

$$\begin{aligned}
\frac{\partial L}{\partial(dx^\gamma/d\lambda)} &= \frac{1}{2L} \frac{\partial L'}{\partial(dx^\gamma/d\lambda)} \\
&= \frac{1}{2L} \frac{\partial}{\partial(dx^\gamma/d\lambda)} \left(g_{\alpha\beta} \frac{dx^\alpha}{d\lambda} \frac{dx^\beta}{d\lambda} \right) \\
&= \frac{1}{2L} g_{\alpha\beta} \frac{\partial}{\partial(dx^\gamma/d\lambda)} \left(\frac{dx^\alpha}{d\lambda} \frac{dx^\beta}{d\lambda} \right) \\
&= \frac{1}{2L} g_{\alpha\beta} \left(\frac{dx^\beta}{d\lambda} \frac{\partial dx^\alpha/d\lambda}{\partial dx^\gamma/d\lambda} + \frac{dx^\alpha}{d\lambda} \frac{\partial dx^\beta/d\lambda}{\partial dx^\gamma/d\lambda} \right) \\
&= \frac{1}{2L} g_{\alpha\beta} \left(\frac{dx^\beta}{d\lambda} \delta_{\alpha\gamma} + \frac{dx^\alpha}{d\lambda} \delta_{\beta\gamma} \right) \\
&= \frac{1}{2L} \left(g_{\gamma\beta} \frac{dx^\beta}{d\lambda} + g_{\alpha\gamma} \frac{dx^\alpha}{d\lambda} \right) \\
&= \frac{1}{2L} \left(g_{\alpha\gamma} \frac{dx^\alpha}{d\lambda} + g_{\alpha\gamma} \frac{dx^\alpha}{d\lambda} \right) \\
&= \frac{1}{2L} \left(2g_{\alpha\gamma} \frac{dx^\alpha}{d\lambda} \right) \\
&= \frac{1}{L} g_{\alpha\gamma} \frac{dx^\alpha}{d\lambda}. \tag{D.8}
\end{aligned}$$

Now I still need to take the derivative of equation (D.8) with respect to λ :

$$\begin{aligned}
\frac{d}{d\lambda} \left(\frac{\partial L}{\partial(dx^\gamma/d\lambda)} \right) &= \frac{d}{d\lambda} \left(\frac{1}{L} g_{\alpha\gamma} \frac{dx^\alpha}{d\lambda} \right) = \frac{1}{L} \frac{d}{d\lambda} \left(g_{\alpha\gamma} \frac{dx^\alpha}{d\lambda} \right) \\
&= \frac{1}{L} \left(g_{\alpha\gamma} \frac{d^2 x^\alpha}{d\lambda^2} + \frac{dx^\alpha}{d\lambda} \frac{dg_{\alpha\gamma}}{d\lambda} \right) \\
&= \frac{1}{L} \left(g_{\alpha\gamma} \frac{d^2 x^\alpha}{d\lambda^2} + \frac{dx^\alpha}{d\lambda} \frac{dg_{\alpha\gamma}}{dx^\beta} \frac{dx^\beta}{d\lambda} \right), \\
\frac{dg_{\alpha\gamma}}{dx^\beta} &= \frac{1}{2} \left(\frac{dg_{\alpha\gamma}}{dx^\beta} + \frac{dg_{\alpha\gamma}}{dx^\beta} \right) = \frac{1}{2} \left(\frac{dg_{\alpha\gamma}}{dx^\beta} + \frac{dg_{\gamma\beta}}{dx^\alpha} \right) \Rightarrow \\
\frac{d}{d\lambda} \left(\frac{\partial L}{\partial(dx^\gamma/d\lambda)} \right) &= \frac{1}{L} \left(g_{\alpha\gamma} \frac{d^2 x^\alpha}{d\lambda^2} + \frac{1}{2} \left(\frac{dg_{\alpha\gamma}}{dx^\beta} + \frac{dg_{\gamma\beta}}{dx^\alpha} \right) \frac{dx^\alpha}{d\lambda} \frac{dx^\beta}{d\lambda} \right) \tag{D.9}
\end{aligned}$$

The second term in equation (D.7):

$$\begin{aligned}
\frac{\partial L}{\partial x^\gamma} &= \frac{1}{2L} \frac{\partial L'}{\partial x^\gamma} \\
&= \frac{1}{2L} \frac{\partial}{\partial x^\gamma} \left(g_{\alpha\beta} \frac{dx^\alpha}{d\lambda} \frac{dx^\beta}{d\lambda} \right) \\
&= \frac{1}{2L} \frac{\partial g_{\alpha\beta}}{\partial x^\gamma} \frac{dx^\alpha}{d\lambda} \frac{dx^\beta}{d\lambda}
\end{aligned} \tag{D.10}$$

Substituting the equations (D.9) and (D.10) into equation (D.7), yields

$$\begin{aligned}
0 &= \frac{1}{L} \left(g_{\alpha\gamma} \frac{d^2 x^\alpha}{d\lambda^2} + \frac{1}{2} \left(\frac{dg_{\alpha\gamma}}{dx^\beta} + \frac{dg_{\gamma\beta}}{dx^\alpha} \right) \frac{dx^\alpha}{d\lambda} \frac{dx^\beta}{d\lambda} \right) - \frac{1}{2L} \frac{\partial g_{\alpha\beta}}{\partial x^\gamma} \frac{dx^\alpha}{d\lambda} \frac{dx^\beta}{d\lambda} \\
&= g_{\alpha\gamma} \frac{d^2 x^\alpha}{d\lambda^2} + \frac{1}{2} \left(\frac{dg_{\alpha\gamma}}{dx^\beta} + \frac{dg_{\gamma\beta}}{dx^\alpha} \right) \frac{dx^\alpha}{d\lambda} \frac{dx^\beta}{d\lambda} - \frac{1}{2} \frac{\partial g_{\alpha\beta}}{\partial x^\gamma} \frac{dx^\alpha}{d\lambda} \frac{dx^\beta}{d\lambda} \Rightarrow \\
g_{\alpha\gamma} \frac{d^2 x^\alpha}{d\lambda^2} &= \frac{1}{2} \frac{\partial g_{\alpha\beta}}{\partial x^\gamma} \frac{dx^\alpha}{d\lambda} \frac{dx^\beta}{d\lambda} - \frac{1}{2} \left(\frac{dg_{\alpha\gamma}}{dx^\beta} + \frac{dg_{\gamma\beta}}{dx^\alpha} \right) \frac{dx^\alpha}{d\lambda} \frac{dx^\beta}{d\lambda} \\
&= -\frac{1}{2} \left(\frac{dg_{\alpha\gamma}}{dx^\beta} + \frac{dg_{\gamma\beta}}{dx^\alpha} - \frac{\partial g_{\alpha\beta}}{\partial x^\gamma} \right) \frac{dx^\alpha}{d\lambda} \frac{dx^\beta}{d\lambda} \\
&= -\frac{1}{2} \left(\frac{dg_{\delta\gamma}}{dx^\beta} + \frac{dg_{\gamma\beta}}{dx^\delta} - \frac{\partial g_{\delta\beta}}{\partial x^\gamma} \right) \frac{dx^\delta}{d\lambda} \frac{dx^\beta}{d\lambda}.
\end{aligned} \tag{D.11}$$

Now it is time to introduce the Christoffel symbol given by

$$\Gamma_{\delta\beta}^\alpha = \frac{1}{2} g^{\alpha\gamma} \left(\frac{dg_{\delta\gamma}}{dx^\beta} + \frac{dg_{\gamma\beta}}{dx^\delta} - \frac{\partial g_{\delta\beta}}{\partial x^\gamma} \right). \tag{D.12}$$

Since $g^{\alpha\gamma} = (g_{\alpha\gamma})^{-1}$, equation (D.12) allows me to write

$$g_{\alpha\gamma} \Gamma_{\delta\beta}^\alpha = \frac{1}{2} \left(\frac{dg_{\delta\gamma}}{dx^\beta} + \frac{dg_{\gamma\beta}}{dx^\delta} - \frac{\partial g_{\delta\beta}}{\partial x^\gamma} \right). \tag{D.13}$$

Substituting equation (D.13) into equation (D.11) yields

$$\begin{aligned}
g_{\alpha\gamma} \frac{d^2 x^\alpha}{d\lambda^2} &= -g_{\alpha\gamma} \Gamma_{\delta\beta}^\alpha \frac{dx^\delta}{d\lambda} \frac{dx^\beta}{d\lambda} \Rightarrow \\
\frac{d^2 x^\alpha}{d\lambda^2} &= -\Gamma_{\delta\beta}^\alpha \frac{dx^\delta}{d\lambda} \frac{dx^\beta}{d\lambda} \Rightarrow \\
\frac{d^2 x^\alpha}{d\lambda^2} + \Gamma_{\delta\beta}^\alpha \frac{dx^\delta}{d\lambda} \frac{dx^\beta}{d\lambda} &= 0.
\end{aligned} \tag{D.14}$$

Equation (D.14) is known as the Geodesic equation - the generalization of the notion of a straight line to curved spacetime. As required, the geodesic equation reduces to that of a straight line, $\frac{d^2 x^\alpha}{d\lambda^2} = 0$, in flat spacetime, because in this case, all components of the Christoffel symbol vanish, since all derivatives of the metric tensor, $g_{\mu\nu}$, vanish.

E

In this appendix, I provide a derivation of the equation of hydrostatic equilibrium given by equation (3.2) and the generalized equation including radial streaming motions and time dependence given by equation (3.9). I start out with the Euler equation given by

$$\frac{\partial \mathbf{v}}{\partial t} + (\mathbf{v} \cdot \nabla) \mathbf{v} = -\frac{1}{\rho} \nabla P - \nabla \Phi. \quad (\text{E.1})$$

The variables are explained in section 3.1.

The equation of hydrostatic equilibrium

A system in hydrostatic equilibrium is a steady state system, which means that time gradients vanish, and thereby the first term on the LHS of equation (E.1) vanishes. For simplicity, it is furthermore assumed that the system is spherically symmetric, whereby all angular gradients vanish, and thus the spatial gradient, ∇ , reduces to the radial gradient, ∂_r . In addition, a system in hydrostatic equilibrium is characterized by the property that the internal gas pressure pushing the gas outwards exactly cancels the self-gravity of the system. In this case, there are no net radial streaming motions, i.e. $\bar{v}_r = 0$, and thus the second term on the LHS of equation (E.1) also vanishes.¹¹ Therefore, using these assumptions, equation (E.1) reduces to

$$\frac{\partial \Phi(r)}{\partial r} = -\frac{1}{\rho} \frac{\partial P}{\partial r}. \quad (\text{E.2})$$

Meanwhile, assuming that the gas in the system can be regarded as an ideal gas, the gas pressure, P , can be related to the gas density, ρ , and the gas tem-

¹¹In order for this derivation to be consistent with the derivation of the Jeans equation in appendix F, it is also assumed that there are no net rotational streaming motions, i.e. $\bar{v}_\theta = \bar{v}_\phi = 0$. This has no immediate influence, since the two terms on the LHS of equation (E.1) have already vanished due to our assumptions of a steady state and spherical symmetry.

perature, T , by the ideal gas law given by

$$P = \frac{k_B \rho T}{\mu m_H}, \quad (\text{E.3})$$

where k_B is the Boltzmann constant, μ is the mean molecular weight, and m_H is the mass of a hydrogen atom. Substituting equation (E.3) into equation (E.2) yields

$$\frac{\partial \Phi}{\partial r} = -\frac{1}{\rho} \frac{k_B}{\mu m_H} \frac{\partial}{\partial r} (\rho T), \quad (\text{E.4})$$

and using the relation, $\frac{\partial a}{\partial b} = \frac{a}{b} \frac{\partial \ln a}{\partial \ln b}$, I get

$$\frac{\partial \Phi(r)}{\partial r} = -\frac{k_B}{\mu m_H} \frac{\rho T}{\rho r} \frac{\partial \ln(\rho T)}{\partial \ln r} = -\frac{k_B T}{\mu m_H r} \left(\frac{\partial \ln \rho}{\partial \ln r} + \frac{\partial \ln T}{\partial \ln r} \right). \quad (\text{E.5})$$

As the last thing, I assume that the system is subject to its own gravitation only, and thereby gravitational contributions from the underlying cosmology of the universe (i.e. contributions from the background density and the cosmological constant) are neglected. This means that $\frac{\partial \Phi(r)}{\partial r} = \frac{GM(r)}{r^2}$, and thus I arrive at equation (3.2); the equation of hydrostatic equilibrium given by

$$\frac{\partial \Phi(r)}{\partial r} = \frac{GM(r)}{r^2} = -\frac{k_B T}{\mu m_H r} \left(\frac{\partial \ln \rho}{\partial \ln r} + \frac{\partial \ln T}{\partial \ln r} \right). \quad (\text{E.6})$$

The generalized equation

Now to the generalized version of equation (3.2) given by equation (3.9). If one retains the mean radial velocity component, \bar{v}_r , and time derivatives, ∂_t , i.e. if one does not neglect radial streaming motions (hydrostatic equilibrium) and time dependence, the two terms on the LHS of equation (E.1) can no longer be ignored. However, spherical symmetry will still be assumed (i.e. $\nabla = \partial_r$). In this case, the RHS of equation (E.1) can be written in the form of equation (E.5), so in total, equation (E.1) now reads

$$\begin{aligned} \frac{\partial \bar{v}_r}{\partial t} + \bar{v}_r \frac{\partial \bar{v}_r}{\partial r} &= -\frac{\partial \Phi(r)}{\partial r} - \frac{k_B T}{\mu m_H r} \left(\frac{\partial \ln \rho}{\partial \ln r} + \frac{\partial \ln T}{\partial \ln r} \right) \quad => \\ \frac{\partial \Phi(r)}{\partial r} &= -\frac{k_B T}{\mu m_H r} \left(\frac{\partial \ln \rho}{\partial \ln r} + \frac{\partial \ln T}{\partial \ln r} \right) - \left(\bar{v}_r \frac{\partial \bar{v}_r}{\partial r} + \frac{\partial \bar{v}_r}{\partial t} \right). \end{aligned} \quad (\text{E.7})$$

Moreover, the mean radial velocity is the sum of the peculiar velocity component, \bar{v}_p , and the Hubble flow given by Hr , so $\bar{v}_r = \bar{v}_p + Hr$. Using this expression, the last term in equation (E.7) can be rewritten as

$$\begin{aligned}
\bar{v}_r \frac{\partial \bar{v}_r}{\partial r} + \frac{\partial \bar{v}_r}{\partial t} &= (\bar{v}_p + Hr) \frac{\partial}{\partial r} (\bar{v}_p + Hr) + \frac{\partial}{\partial t} (\bar{v}_p + Hr) \\
&= (\bar{v}_p + Hr) \left(\frac{\partial \bar{v}_p}{\partial r} + H \right) + \frac{\partial \bar{v}_p}{\partial t} + \frac{\partial}{\partial t} (Hr) \\
&= \bar{v}_p \frac{\partial \bar{v}_p}{\partial r} + H \bar{v}_p + Hr \frac{\partial \bar{v}_p}{\partial r} + H^2 r + \frac{\partial \bar{v}_p}{\partial t} + r \frac{\partial H}{\partial t} \\
&= \bar{v}_p \frac{\partial \bar{v}_p}{\partial r} + H \left(\bar{v}_p + r \frac{\partial \bar{v}_p}{\partial r} \right) + \frac{\partial \bar{v}_p}{\partial t} + r(H^2 + \dot{H}). \tag{E.8}
\end{aligned}$$

Meanwhile, I have that

$$\dot{H} = -(1+q)H^2 \quad \Rightarrow \quad r(H^2 + \dot{H}) = -qH^2 r, \tag{E.9}$$

where q is the deceleration parameter. Substituting equation (E.9) into equation (E.8) yields

$$\bar{v}_r \frac{\partial \bar{v}_r}{\partial r} + \frac{\partial \bar{v}_r}{\partial t} = \bar{v}_p \frac{\partial \bar{v}_p}{\partial r} + H \left(\bar{v}_p + r \frac{\partial \bar{v}_p}{\partial r} \right) - qH^2 r + \frac{\partial \bar{v}_p}{\partial t}. \tag{E.10}$$

Thus, equation (E.7) can now be written

$$\begin{aligned}
\frac{\partial \Phi(r)}{\partial r} &= -\frac{k_B T}{\mu m_H r} \left(\frac{\partial \ln \rho}{\partial \ln r} + \frac{\partial \ln T}{\partial \ln r} \right) - \left(\bar{v}_r \frac{\partial \bar{v}_r}{\partial r} + \frac{\partial \bar{v}_r}{\partial t} \right) \\
&= -\frac{k_B T}{\mu m_H r} \left(\frac{\partial \ln \rho}{\partial \ln r} + \frac{\partial \ln T}{\partial \ln r} \right) \\
&\quad - \left(\bar{v}_p \frac{\partial \bar{v}_p}{\partial r} + H \left(\bar{v}_p + r \frac{\partial \bar{v}_p}{\partial r} \right) - qH^2 r + \frac{\partial \bar{v}_p}{\partial t} \right), \tag{E.11}
\end{aligned}$$

which is identical to equation (3.7).

As mentioned in section 3.2, since I am considering relatively large distances, the underlying cosmology of our universe should be taken into account. When doing this, the total gravitational potential is given by equation (3.8) (rewritten here for convenience):

$$\frac{\partial \Phi(r)}{\partial r} = \frac{GM(r)}{r^2} + \frac{4\pi}{3} G \rho_b r - \frac{1}{3} \Lambda r, \tag{E.12}$$

where ρ_b is the background density of the universe, and Λ is the cosmological constant. The first term is the system's own gravitational potential, while the second and third terms are the potential resulting from the background density and that resulting from the cosmological constant respectively. Now it is time to introduce the dimensionless density parameters of the background density and the cosmological constant given by respectively,

$$\Omega_m = \frac{8\pi G\rho_b}{3H^2}, \quad \Omega_\Lambda = \frac{\Lambda}{3H^2}. \quad (\text{E.13})$$

Solving these expressions for ρ_b and Λ yields

$$\rho_b = \frac{3H^2\Omega_m}{8\pi G}, \quad \Lambda = 3H^2\Omega_\Lambda, \quad (\text{E.14})$$

and substituting this into equation (E.12) gives

$$\begin{aligned} \frac{\partial\Phi(r)}{\partial r} &= \frac{GM(r)}{r^2} + \frac{1}{2}H^2r\Omega_m - H^2r\Omega_\Lambda \\ &= \frac{GM(r)}{r^2} + H^2r\left(\frac{1}{2}\Omega_m - \Omega_\Lambda\right) \\ &= \frac{GM(r)}{r^2} + qH^2r, \end{aligned} \quad (\text{E.15})$$

where I have used that $q = \frac{1}{2}\Omega_m - \Omega_\Lambda$. Now substituting equation (E.15) into equation (E.11), I recover equation (3.9):

$$\begin{aligned} \frac{GM(r)}{r^2} &= -\frac{k_BT}{\mu m_H r} \left(\frac{\partial \ln \rho}{\partial \ln r} + \frac{\partial \ln T}{\partial \ln r} \right) - \left(\bar{v}_r \frac{\partial \bar{v}_r}{\partial r} + \frac{\partial \bar{v}_r}{\partial t} \right) - qH^2r \\ &= -\frac{k_BT}{\mu m_H r} \left(\frac{\partial \ln \rho}{\partial \ln r} + \frac{\partial \ln T}{\partial \ln r} \right) \\ &\quad - \left(\bar{v}_p \frac{\partial \bar{v}_p}{\partial r} + H \left(\bar{v}_p + r \frac{\partial \bar{v}_p}{\partial r} \right) + \frac{\partial \bar{v}_p}{\partial t} \right). \end{aligned} \quad (\text{E.16})$$

F

In this appendix, I provide a derivation of the standard Jeans equation given by equation (3.6) and the generalized Jeans equation including radial streaming motions and time dependence given by equation (3.10).

The standard Jeans equation

I start out with the collisionless Boltzmann equation given by

$$\begin{aligned} \frac{\partial f}{\partial t} + p_r \frac{\partial f}{\partial r} + \frac{p_\theta}{r^2} \frac{\partial f}{\partial \theta} + \frac{p_\phi}{r^2 \sin^2 \theta} \frac{\partial f}{\partial \phi} - \left(\frac{\partial \Phi}{\partial r} - \frac{p_\theta^2}{r^3} - \frac{p_\phi^2}{r^3 \sin^2 \theta} \right) \frac{\partial f}{\partial p_r} \\ - \left(\frac{\partial \Phi}{\partial \theta} - \frac{p_\phi^2 \cos \theta}{r^2 \sin^3 \theta} \right) \frac{\partial f}{\partial p_\theta} - \frac{\partial \Phi}{\partial \phi} \frac{\partial f}{\partial p_\phi} = 0. \end{aligned} \quad (\text{F.1})$$

The variables are explained in section 3.1. Assuming that I am dealing with a spherical and time-independent system, terms involving ∂_t , ∂_θ and ∂_ϕ can be dropped, and so equation (F.1) reduces to

$$p_r \frac{\partial f}{\partial r} - \left(\frac{\partial \Phi}{\partial r} - \frac{p_\theta^2}{r^3} - \frac{p_\phi^2}{r^3 \sin^2 \theta} \right) \frac{\partial f}{\partial p_r} - \frac{p_\phi^2 \cos \theta}{r^2 \sin^3 \theta} \frac{\partial f}{\partial p_\theta} = 0. \quad (\text{F.2})$$

I multiply equation (F.2) by $p_r dp_r dp_\theta dp_\phi$ and integrate over all momenta using the relation $\int dp_r dp_\theta dp_\phi f = r^2 \sin \theta \nu$. I first consider the leftmost term on the LHS of equation (F.2):

$$\begin{aligned} p_r \frac{\partial}{\partial r} \left(\int p_r dp_r dp_\theta dp_\phi f \right) &= \frac{\partial}{\partial r} \left(\overline{p_r^2} r^2 \sin \theta \nu \right) = \sin \theta \frac{\partial}{\partial r} \left(\nu r^2 \overline{p_r^2} \right) \\ &= \sin \theta \left(r^2 \frac{\partial}{\partial r} \left(\nu \overline{p_r^2} \right) + \nu \overline{p_r^2} \frac{\partial r^2}{\partial r} \right) \\ &= r^2 \sin \theta \frac{\partial}{\partial r} (\nu \overline{p_r^2}) + 2r \sin \theta \nu \overline{p_r^2}. \end{aligned} \quad (\text{F.3})$$

The middle term on the LHS of equation (F.2):

$$\begin{aligned} \frac{\partial}{\partial p_r} \left(\int p_r dp_r dp_\theta dp_\phi f \right) &= r^2 \sin \theta \nu \quad \Rightarrow \\ \int \left(\frac{\partial \Phi}{\partial r} - \frac{p_\theta^2}{r^3} - \frac{p_\phi^2}{r^3 \sin^2 \theta} \right) \frac{\partial f}{\partial p_r} p_r dp_r dp_\theta dp_\phi &= r^2 \sin \theta \nu \left(\frac{\partial \Phi}{\partial r} - \frac{\overline{p_\theta^2}}{r^3} - \frac{\overline{p_\phi^2}}{r^3 \sin^2 \theta} \right). \end{aligned} \quad (\text{F.4})$$

The rightmost term on the LHS of equation (F.2):

$$\int p_r dp_r dp_\theta dp_\phi p_r \frac{\partial f}{\partial p_\theta} = \frac{\partial}{\partial p_\theta} (\overline{p_r} r^2 \sin \theta \nu) = 0. \quad (\text{F.5})$$

Combining equations (F.3), (F.4) and (F.5) and dividing each term by $r^2 \sin \theta$ yields

$$\frac{\partial}{\partial r}(\nu \overline{p_r^2}) + 2\nu \frac{\overline{p_r^2}}{r} + \nu \left(\frac{\partial \Phi}{\partial r} - \frac{\overline{p_\theta^2}}{r^3} - \frac{\overline{p_\phi^2}}{r^3 \sin^2 \theta} \right) = 0. \quad (\text{F.6})$$

Next I substitute the relations $p_r = v_r$, $p_\theta = r v_\theta$ and $p_\phi = r \sin \theta v_\phi$ (relating the canonical momenta, p_i , to the velocity components, v_i , where $i = r, \theta, \phi$) into equation (F.6). This way, each momentum component gets replaced by the corresponding velocity component, so equation (F.6) becomes

$$\frac{\partial}{\partial r}(\nu \overline{v_r^2}) + 2\nu \frac{\overline{v_r^2}}{r} + \nu \left(\frac{\partial \Phi}{\partial r} - \frac{\overline{v_\theta^2}}{r} - \frac{\overline{v_\phi^2}}{r} \right) = 0. \quad (\text{F.7})$$

Rearranging equation (F.7) and solving for $-\nu \frac{\partial \Phi}{\partial r}$ yields

$$-\nu \frac{\partial \Phi}{\partial r} = \frac{\partial}{\partial r}(\nu \overline{v_r^2}) + \frac{\nu}{r} \left(2\overline{v_r^2} - \overline{v_\theta^2} - \overline{v_\phi^2} \right). \quad (\text{F.8})$$

In general, $\sigma_i^2 = \overline{v_i^2} - \overline{v_i}^2$. Now however, I assume that any net streaming motion can be neglected, i.e. the mean velocity components $\overline{v_i}$ are all set to zero, and therefore I can now write $\sigma_i^2 = \overline{v_i^2}$. Substituting this relation into equation (F.8) gives

$$-\nu \frac{\partial \Phi}{\partial r} = \frac{\partial}{\partial r}(\nu \sigma_r^2) + \frac{\nu}{r} (2\sigma_r^2 - \sigma_\theta^2 - \sigma_\phi^2). \quad (\text{F.9})$$

Now I use the definition of β given by equation (3.5) to get rid of the angular velocity dispersions in the last term on the RHS of equation (F.9):

$$\beta \equiv 1 - \frac{\sigma_\theta^2 + \sigma_\phi^2}{2\sigma_r^2} \quad \Rightarrow \quad 2\beta\sigma_r^2 = 2\sigma_r^2 - \sigma_\theta^2 - \sigma_\phi^2, \quad (\text{F.10})$$

so equation (F.9) now becomes

$$-\nu \frac{\partial \Phi(r)}{\partial r} = \frac{\partial}{\partial r}(\nu \sigma_r^2) + 2\frac{\beta}{r} \nu \sigma_r^2. \quad (\text{F.11})$$

This equation is identical to equation (3.4).

The solution to equation (F.11) that satisfies the boundary condition, $\lim_{r \rightarrow \infty} \sigma^2 = 0$, is

$$\sigma_r^2(r) = \frac{1}{r^{2\beta} \nu(r)} \int_r^\infty r'^{2\beta} \nu(r') \frac{\partial \Phi(r')}{\partial r'} dr'. \quad (\text{F.12})$$

I want to solve equation (F.12) for $\frac{\partial \Phi}{\partial r}$ in order to recover equation (3.6). Starting by multiplying by $r^{2\beta}\nu$ and differentiating with respect to r , I get

$$\frac{\partial}{\partial r} (\sigma_r^2 \nu r^{2\beta}) = -r^{2\beta} \nu \frac{\partial \Phi}{\partial r}, \quad (\text{F.13})$$

where the LHS can be rewritten using the relation $\frac{\partial a}{\partial b} = \frac{a}{b} \frac{\partial \ln a}{\partial \ln b}$:

$$\begin{aligned} \frac{\partial}{\partial r} (\sigma_r^2 \nu r^{2\beta}) &= \nu r^{2\beta} \frac{\partial \sigma_r^2}{\partial r} + \sigma_r^2 r^{2\beta} \frac{\partial \nu}{\partial r} + \nu \sigma_r^2 \frac{\partial r^{2\beta}}{\partial r} \\ &= \nu r^{2\beta} \frac{\sigma_r^2}{r} \frac{\partial \ln \sigma_r^2}{\partial \ln r} + \sigma_r^2 r^{2\beta} \frac{\nu}{r} \frac{\partial \ln \nu}{\partial \ln r} + 2\beta \nu \sigma_r^2 \frac{r^{2\beta}}{r} \\ &= \nu \sigma_r^2 \frac{r^{2\beta}}{r} \left(\frac{\partial \ln \nu}{\partial \ln r} + \frac{\partial \ln \sigma_r^2}{\partial \ln r} + 2\beta \right). \end{aligned} \quad (\text{F.14})$$

Using equation (F.14) and dividing by $\nu \frac{r^{2\beta}}{r}$, equation (F.13) becomes

$$\sigma_r^2 \left(\frac{\partial \ln \nu}{\partial \ln r} + \frac{\partial \ln \sigma_r^2}{\partial \ln r} + 2\beta \right) = -r \frac{\partial \Phi(r)}{\partial r} = -r \frac{GM(r)}{r^2}, \quad (\text{F.15})$$

where it has been assumed that the system is subject to its own gravitation only, i.e. $\frac{\partial \Phi(r)}{\partial r} = \frac{GM(r)}{r^2}$. Dividing equation (F.15) by r , I recover the standard Jeans equation in the form of equation (3.6) given by

$$\frac{\partial \Phi(r)}{\partial r} = \frac{GM(r)}{r^2} = -\frac{\sigma_r^2}{r} \left(\frac{\partial \ln \nu}{\partial \ln r} + \frac{\partial \ln \sigma_r^2}{\partial \ln r} + 2\beta \right). \quad (\text{F.16})$$

The generalized Jeans equation

Now to the generalized Jeans equation given by equation (3.10), where the mean radial velocity component, \bar{v}_r , and time derivatives, ∂_t , will not be ignored. In this case, one has to retain the first (leftmost) term in equation (F.1), while terms involving ∂_θ and ∂_ϕ can still be dropped due to the assumption of spherical symmetry, so equation (F.1) becomes

$$\frac{\partial f}{\partial t} + p_r \frac{\partial f}{\partial r} - \left(\frac{\partial \Phi}{\partial r} - \frac{p_\theta^2}{r^3} - \frac{p_\phi^2}{r^3 \sin^2 \theta} \right) \frac{\partial f}{\partial p_r} - \frac{p_\phi^2 \cos \theta}{r^2 \sin^3 \theta} \frac{\partial f}{\partial p_\theta} = 0. \quad (\text{F.17})$$

The only difference between equation (F.2) and equation (F.17) is the inclusion of the term $\partial f / \partial t$ in equation (F.17). I will now give this term the same treatment

as was given to the other terms in the equation in the derivation of the standard Jeans equation, i.e. it will be multiplied by $p_r dp_r dp_\theta dp_\phi$ and integrated over all momenta using the relation $\int dp_r dp_\theta dp_\phi f = r^2 \sin \theta \nu$. This yields

$$\frac{\partial}{\partial t} \left(\int p_r dp_r dp_\theta dp_\phi f \right) = \frac{\partial}{\partial t} (\bar{p}_r r^2 \sin \theta \nu) = r^2 \sin \theta \frac{\partial}{\partial t} (\nu \bar{p}_r), \quad (\text{F.18})$$

which gives

$$\frac{\partial}{\partial t} (\nu \bar{p}_r) + \frac{\partial}{\partial r} (\nu \bar{p}_r^2) + 2\nu \frac{\bar{p}_r^2}{r} + \nu \left(\frac{\partial \Phi}{\partial r} - \frac{\bar{p}_\theta^2}{r^3} - \frac{\bar{p}_\phi^2}{r^3 \sin^2 \theta} \right) = 0 \quad (\text{F.19})$$

as a replacement for equation (F.6). Again using the relations $p_r = v_r$, $p_\theta = r v_\theta$ and $p_\phi = r \sin \theta v_\phi$ and solving for $-\nu \frac{\partial \Phi}{\partial r}$, equation (F.19) becomes

$$-\nu \frac{\partial \Phi}{\partial r} = \frac{\partial}{\partial t} (\nu \bar{v}_r) + \frac{\partial}{\partial r} (\nu \bar{v}_r^2) + \frac{\nu}{r} (2\bar{v}_r^2 - \bar{v}_\theta^2 - \bar{v}_\phi^2). \quad (\text{F.20})$$

In the derivation of equation (3.6), it was assumed that any net streaming motion can be neglected, i.e. the mean velocity components, \bar{v}_i , are all set to zero. Now however, it will only be assumed that there are no net angular streaming motions (i.e. $\bar{v}_\theta = \bar{v}_\phi = 0$), while \bar{v}_r is retained. This way, I have the relations $\sigma_\theta^2 = \bar{v}_\theta^2$, $\sigma_\phi^2 = \bar{v}_\phi^2$ and $\sigma_r^2 = \bar{v}_r^2 - \bar{v}_r^2 = \sigma_r^2 + \bar{v}_r^2$, which I now substitute into equation (F.20). This yields

$$\begin{aligned} -\nu \frac{\partial \Phi}{\partial r} &= \frac{\partial}{\partial t} (\nu \bar{v}_r) + \frac{\partial}{\partial r} (\nu (\sigma_r^2 + \bar{v}_r^2)) + \frac{\nu}{r} (2(\sigma_r^2 + \bar{v}_r^2) - \sigma_\theta^2 - \sigma_\phi^2) \\ &= \frac{\partial}{\partial t} (\nu \bar{v}_r) + \frac{\partial}{\partial r} (\nu \sigma_r^2) + \frac{\partial}{\partial r} (\nu \bar{v}_r^2) + 2\frac{\nu}{r} \bar{v}_r^2 + \frac{\nu}{r} (2\sigma_r^2 - \sigma_\theta^2 - \sigma_\phi^2) \\ &= \frac{\partial}{\partial t} (\nu \bar{v}_r) + \frac{\partial}{\partial r} (\nu \sigma_r^2) + \frac{\partial}{\partial r} (\nu \bar{v}_r^2) + 2\frac{\nu}{r} \bar{v}_r^2 + 2\beta \frac{\nu}{r} \sigma_r^2, \end{aligned} \quad (\text{F.21})$$

where, at the last equality sign, I have used the definition of β given by equation (F.10).

To get further, I need a generalized version of the continuity equation, and to obtain this, I start by multiplying equation (F.17) by $dp_r dp_\theta dp_\phi$ and then integrate over all momenta. Here, only the first two terms of equation (F.17) will be calculated, since all the other terms vanish when the integration is carried out. The first term on the LHS:

$$\frac{\partial}{\partial t} \left(\int dp_r dp_\theta dp_\phi f \right) = r^2 \sin \theta \frac{\partial \nu}{\partial t}. \quad (\text{F.22})$$

The second term on the LHS:

$$\begin{aligned} p_r \frac{\partial}{\partial r} \left(\int dp_r dp_\theta dp_\phi f \right) &= \sin \theta \frac{\partial}{\partial r} (\nu r^2 \bar{v}_r) = \sin \theta \left(\nu \bar{v}_r \frac{\partial r^2}{\partial r} + r^2 \frac{\partial}{\partial r} (\nu \bar{v}_r) \right) \\ &= r^2 \sin \theta \frac{\partial}{\partial r} (\nu \bar{v}_r) + 2r \sin \theta \nu \bar{v}_r. \end{aligned} \quad (\text{F.23})$$

Combining equations (F.22) and (F.23) and dividing by $r^2 \sin \theta$ gives

$$\frac{\partial \nu}{\partial t} + \frac{\partial}{\partial r} (\nu \bar{v}_r) + 2 \frac{\nu}{r} \bar{v}_r = 0 \quad \Rightarrow \quad \frac{\partial \nu}{\partial t} = - \frac{\partial}{\partial r} (\nu \bar{v}_r) - 2 \frac{\nu}{r} \bar{v}_r, \quad (\text{F.24})$$

so the first term after the last equality sign in equation (F.21) becomes

$$\begin{aligned} \frac{\partial}{\partial t} (\nu \bar{v}_r) &= \bar{v}_r \frac{\partial \nu}{\partial t} + \nu \frac{\partial \bar{v}_r}{\partial t} = - \bar{v}_r \left(\frac{\partial}{\partial r} (\nu \bar{v}_r) + 2 \frac{\nu}{r} \bar{v}_r \right) + \nu \frac{\partial \bar{v}_r}{\partial t} \\ &= - \bar{v}_r \frac{\partial}{\partial r} (\nu \bar{v}_r) - 2 \frac{\nu}{r} \bar{v}_r^2 + \nu \frac{\partial \bar{v}_r}{\partial t}. \end{aligned} \quad (\text{F.25})$$

Substituting equation (F.25) into equation (F.21) yields

$$\begin{aligned} -\nu \frac{\partial \Phi}{\partial r} &= - \bar{v}_r \frac{\partial}{\partial r} (\nu \bar{v}_r) - 2 \frac{\nu}{r} \bar{v}_r^2 + \nu \frac{\partial \bar{v}_r}{\partial t} + \frac{\partial}{\partial r} (\nu \sigma_r^2) + \frac{\partial}{\partial r} (\nu \bar{v}_r^2) + 2 \frac{\nu}{r} \bar{v}_r^2 + 2 \beta \frac{\nu}{r} \sigma_r^2 \\ &= - \bar{v}_r \frac{\partial}{\partial r} (\nu \bar{v}_r) + \nu \frac{\partial \bar{v}_r}{\partial t} + \frac{\partial}{\partial r} (\nu \sigma_r^2) + \frac{\partial}{\partial r} (\nu \bar{v}_r^2) + 2 \beta \frac{\nu}{r} \sigma_r^2. \end{aligned} \quad (\text{F.26})$$

Now I look at the first and the fourth term after the last equality sign in equation (F.26), starting with the first:

$$\bar{v}_r \frac{\partial}{\partial r} (\nu \bar{v}_r) = \nu \bar{v}_r \frac{\partial \bar{v}_r}{\partial r} + \bar{v}_r^2 \frac{\partial \nu}{\partial r}. \quad (\text{F.27})$$

And now the fourth term:

$$\frac{\partial}{\partial r} (\nu \bar{v}_r^2) = \nu \frac{\partial \bar{v}_r^2}{\partial r} + \bar{v}_r^2 \frac{\partial \nu}{\partial r} = \nu \left(\bar{v}_r \frac{\partial \bar{v}_r}{\partial r} + \bar{v}_r \frac{\partial \bar{v}_r}{\partial r} \right) + \bar{v}_r^2 \frac{\partial \nu}{\partial r} = 2 \nu \bar{v}_r \frac{\partial \bar{v}_r}{\partial r} + \bar{v}_r^2 \frac{\partial \nu}{\partial r}. \quad (\text{F.28})$$

Subtracting equation (F.27) from equation (F.28) yields

$$2 \nu \bar{v}_r \frac{\partial \bar{v}_r}{\partial r} + \bar{v}_r^2 \frac{\partial \nu}{\partial r} - \left(\nu \bar{v}_r \frac{\partial \bar{v}_r}{\partial r} + \bar{v}_r^2 \frac{\partial \nu}{\partial r} \right) = \nu \bar{v}_r \frac{\partial \bar{v}_r}{\partial r}, \quad (\text{F.29})$$

so equation (F.26) now reads

$$\begin{aligned} -\nu \frac{\partial \Phi}{\partial r} &= \nu \frac{\partial \bar{v}_r}{\partial t} + \frac{\partial}{\partial r} (\nu \sigma_r^2) + \nu \bar{v}_r \frac{\partial \bar{v}_r}{\partial r} + 2 \beta \frac{\nu}{r} \sigma_r^2 \\ &= \frac{\partial}{\partial r} (\nu \sigma_r^2) + 2 \beta \frac{\nu}{r} \sigma_r^2 + \nu \left(\bar{v}_r \frac{\partial \bar{v}_r}{\partial r} + \frac{\partial \bar{v}_r}{\partial t} \right). \end{aligned} \quad (\text{F.30})$$

Equation (F.30) is one way to write the generalized Jeans equation. The difference between the standard and the generalized Jeans equation given by equations (F.16) and (F.30) respectively, is the term, $\nu \left(\bar{v}_r \frac{\partial \bar{v}_r}{\partial r} + \frac{\partial \bar{v}_r}{\partial t} \right)$, that has been "added" to the generalized version. The solution to equation (F.30) that satisfies the boundary condition, $\lim_{r \rightarrow \infty} \sigma^2 = 0$, is

$$\sigma_r^2(r) = \frac{1}{r^{2\beta} \nu(r)} \int_r^\infty r'^{2\beta} \nu(r') \left(\frac{\partial \Phi(r')}{\partial r'} + \bar{v}_{r'} \frac{\partial \bar{v}_{r'}}{\partial r'} + \frac{\partial \bar{v}_{r'}}{\partial t} \right) dr'. \quad (\text{F.31})$$

As in the derivation of the standard Jeans equation, I multiply this by $r^{2\beta} \nu$ and differentiate with respect to r , which yields

$$\frac{\partial}{\partial r} (\sigma_r^2 \nu r^{2\beta}) = -r^{2\beta} \nu \left(\frac{\partial \Phi}{\partial r} + \bar{v}_r \frac{\partial \bar{v}_r}{\partial r} + \frac{\partial \bar{v}_r}{\partial t} \right). \quad (\text{F.32})$$

Using equation (F.14) to rewrite the LHS and dividing by $\nu \frac{r^{2\beta}}{r}$, equation (F.32) becomes

$$\sigma_r^2 \left(\frac{\partial \ln \nu}{\partial \ln r} + \frac{\partial \ln \sigma_r^2}{\partial \ln r} + 2\beta \right) = -r \left(\frac{\partial \Phi}{\partial r} + \bar{v}_r \frac{\partial \bar{v}_r}{\partial r} + \frac{\partial \bar{v}_r}{\partial t} \right) \quad (\text{F.33})$$

Furthermore, including contributions from the underlying cosmology of the universe to the gravitational potential, i.e. using equation (E.12) for the gravitational potential gradient and solving for GM/r^2 , I finally recover the generalized Jeans equation in the form of equation (3.10):

$$\begin{aligned} \frac{GM(r)}{r^2} &= -\frac{\sigma_r^2}{r} \left(\frac{\partial \ln \nu}{\partial \ln r} + \frac{\partial \ln \sigma_r^2}{\partial \ln r} + 2\beta \right) - \left(\tilde{v}_r \frac{\partial \tilde{v}_r}{\partial r} + \frac{\partial \tilde{v}_r}{\partial t} \right) - qH^2 r \\ &= -\frac{\sigma_r^2}{r} \left(\frac{\partial \ln \nu}{\partial \ln r} + \frac{\partial \ln \sigma_r^2}{\partial \ln r} + 2\beta \right) \\ &\quad - \left(\tilde{v}_p \frac{\partial \tilde{v}_p}{\partial r} + H \left(\tilde{v}_p + r \frac{\partial \tilde{v}_p}{\partial r} \right) + \frac{\partial \tilde{v}_p}{\partial t} \right). \end{aligned} \quad (\text{F.34})$$

Note that I have swapped the bar with a tilde when writing the mean radial and peculiar velocity in equation (F.34) in order to clarify that the DM velocity is in general different from the gas velocity.

G

In this appendix, I provide a derivation of equation (3.18) to equation (3.23) (section 3.6). I start out with the generalized Jeans equation given by

$$\frac{GM(r)}{r^2} = -\frac{\sigma_r^2}{r} \left(\frac{\partial \ln \nu}{\partial \ln r} + \frac{\partial \ln \sigma_r^2}{\partial \ln r} + 2\beta \right) - \tilde{F}(r, t), \quad (\text{G.1})$$

where

$$\tilde{F}(r, t) = \left(\tilde{v}_r \frac{\partial \tilde{v}_r}{\partial r} + \frac{\partial \tilde{v}_r}{\partial t} \right) + qH^2 r = \left(\tilde{v}_p \frac{\partial \tilde{v}_p}{\partial r} + H \left(\tilde{v}_p + r \frac{\partial \tilde{v}_p}{\partial r} \right) + \frac{\partial \tilde{v}_p}{\partial t} \right). \quad (\text{G.2})$$

Multiplying equation (G.1) by r gives

$$\frac{GM(r)}{r} = -\sigma_r^2 \left(\frac{\partial \ln \nu}{\partial \ln r} + \frac{\partial \ln \sigma_r^2}{\partial \ln r} + 2\beta \right) - r\tilde{F}(r, t). \quad (\text{G.3})$$

Now I assume that the tangential velocity dispersions are equal, i.e. that $\sigma_\theta = \sigma_\phi = \sigma_t$, which means that the anisotropy parameter is given by

$$\beta = 1 - \frac{\sigma_t^2}{\sigma_r^2}. \quad (\text{G.4})$$

Substituting this expression into equation (G.3) yields

$$\begin{aligned} \frac{GM(r)}{r} &= -\sigma_r^2 \left(\frac{\partial \ln \nu}{\partial \ln r} + \frac{\partial \ln \sigma_r^2}{\partial \ln r} + 2 \left(1 - \frac{\sigma_t^2}{\sigma_r^2} \right) \right) - r\tilde{F}(r, t) \\ &= -\sigma_r^2 \left(\frac{\partial \ln \nu}{\partial \ln r} + \frac{\partial \ln \sigma_r^2}{\partial \ln r} \right) - 2\sigma_r^2 + 2\sigma_t^2 - r\tilde{F}(r, t). \end{aligned} \quad (\text{G.5})$$

Meanwhile, the DM temperature was defined as (equation (3.16))

$$T_{\text{DM}} \equiv \frac{\mu m_H}{k_B} \frac{1}{3} (\sigma_r^2 + \sigma_\theta^2 + \sigma_\phi^2) = \frac{\mu m_H}{3k_B} (\sigma_r^2 + 2\sigma_t^2). \quad (\text{G.6})$$

This can be rewritten as

$$2\sigma_t^2 = \frac{3k_B T_{\text{DM}}}{\mu m_H} - \sigma_r^2, \quad (\text{G.7})$$

and using this expression, equation (G.5) reads

$$\begin{aligned} \frac{GM(r)}{r} &= -\sigma_r^2 \left(\frac{\partial \ln \nu}{\partial \ln r} + \frac{\partial \ln \sigma_r^2}{\partial \ln r} \right) - 2\sigma_r^2 + \frac{3k_B T_{\text{DM}}}{\mu m_H} - \sigma_r^2 - r\tilde{F}(r, t) \\ &= -\sigma_r^2 \left(\frac{\partial \ln \nu}{\partial \ln r} + \frac{\partial \ln \sigma_r^2}{\partial \ln r} + 3 \right) + \frac{3k_B T_{\text{DM}}}{\mu m_H} - r\tilde{F}(r, t). \end{aligned} \quad (\text{G.8})$$

Equation (G.8) can be rewritten as

$$\sigma_r^2 \left(\frac{\partial \ln \nu}{\partial \ln r} + \frac{\partial \ln \sigma_r^2}{\partial \ln r} + 3 \right) = \psi(r, t), \quad (\text{G.9})$$

where

$$\psi(r, t) = \frac{3k_B T_{\text{DM}}}{\mu m_H} - \frac{GM(r)}{r} - r\tilde{F}(r, t). \quad (\text{G.10})$$

Equations (G.9) and (G.10) are identical to equations (3.18) and (3.19) respectively.

Now I will show that equation (3.21) given by

$$\sigma_r^2(r) = \frac{1}{\nu(r)r^3} \int_0^r \psi(r')\nu(r')r'^2 dr' \quad (\text{G.11})$$

is a solution to equation (3.18) (equation (G.9)). Rewriting equation (G.11) and differentiating with respect to r yields

$$\frac{\partial}{\partial r}(\nu r^3 \sigma_r^2) = \psi \nu r^2. \quad (\text{G.12})$$

Next, I rewrite the LHS of equation (G.12) using the relation $\frac{\partial a}{\partial b} = \frac{a}{b} \frac{\partial \ln a}{\partial \ln b}$:

$$\begin{aligned} \frac{\partial}{\partial r}(\nu r^3 \sigma_r^2) &= r^3 \sigma_r^2 \frac{\partial \nu}{\partial r} + \nu \sigma_r^2 \frac{\partial r^3}{\partial r} + \nu r^3 \frac{\partial \sigma_r^2}{\partial r} \\ &= r^3 \sigma_r^2 \frac{\nu}{r} \frac{\partial \ln \nu}{\partial \ln r} + 3r^2 \nu \sigma_r^2 + \nu r^3 \frac{\sigma_r^2}{r} \frac{\partial \ln \sigma_r^2}{\partial \ln r} \\ &= r^2 \nu \sigma_r^2 \left(\frac{\partial \ln \nu}{\partial \ln r} + \frac{\partial \ln \sigma_r^2}{\partial \ln r} + 3 \right). \end{aligned} \quad (\text{G.13})$$

Substituting equation (G.13) back into equation (G.12) and dividing by νr^2 , I get

$$\sigma_r^2 \left(\frac{\partial \ln \nu}{\partial \ln r} + \frac{\partial \ln \sigma_r^2}{\partial \ln r} + 3 \right) = \psi(r, t), \quad (\text{G.14})$$

which is identical to equation (3.18) (equation (G.9)).

Now I proceed to the derivations of the two expressions for the anisotropy parameter, β , given by equations (3.22) and (3.23) starting with the former. Substituting equation (G.7) into equation (G.4) and using that $T_{\text{DM}} = \kappa T_{\text{gas}}$ yields

$$\begin{aligned} \beta &= 1 - \frac{1}{2\sigma_r^2} \left(\frac{3k_B T_{\text{DM}}}{\mu m_H} - \sigma_r^2 \right) = 1 - \frac{3k_B T_{\text{DM}}}{2\mu m_H \sigma_r^2} + \frac{1}{2} = \frac{3}{2} \left(1 - \frac{k_B T_{\text{DM}}}{\mu m_H \sigma_r^2} \right) \\ &= \frac{3}{2} \left(1 - \kappa \frac{k_B T_{\text{gas}}}{\mu m_H \sigma_r^2} \right), \end{aligned} \quad (\text{G.15})$$

which is identical to equation (3.22). Meanwhile, solving the general Jeans equation given by equation (3.10) for β , directly yields equation (3.23) given by

$$\beta = -\frac{1}{2} \left(\frac{\partial \ln \nu}{\partial \ln r} + \frac{\partial \ln \sigma_r^2}{\partial \ln r} + \frac{GM(r)}{r\sigma_r^2} + \frac{r}{\sigma_r^2} \tilde{F}(r, t) \right). \quad (\text{G.16})$$